NASA TECHNICAL MEMORANDUM

NASA TM X-2573

NASA TM X-2573

INTERNAL PERFORMANCE OF A 10° CONICAL PLUG NOZZLE WITH A MULTISPOKE PRIMARY AND TRANSLATING EXTERNAL SHROUD

by Donald L. Bresnahan

Lewis Research Center
Cleveland, Ohio 44135

NATIONAL AERONAUTICS AND SPACE ADMINISTRATION • WASHINGTON, D. C. • JUNE 1972

1 Report No	2 Government Accession No	3. Recipient's Catalog No
NASA TM X-2573		

4. Title and Subtitle	5 Report Date
INTERNAL PERFORMANCE OF A 10^{O} CONICAL PLUG NOZZLE WITH A MULTISPOKE PRIMARY AND TRANSLATING EXTERNAL SHROUD	June 1972
	6 Performing Organization Code
7 Author(s)	8 Performing Organization Report No
Donald L. Bresnahan	E-6877
	10 Work Unit No
9 Performing Organization Name and Address	764-74
Lewis Research Center	11 Contract or Grant No
National Aeronautics and Space Administration	
Cleveland, Ohio 44135	13 Type of Report and Period Covered
12 Sponsoring Agency Name and Address	Technical Memorandum
National Aeronautics and Space Administration	14 Sponsoring Agency Code
Washington, D.C. 20546	

15 Supplementary Notes

16 Abstract

An experimental investigation was conducted in the Lewis Research Center's nozzle static test facility to determine the performance characteristics of a cold-flow, 21.59-centimeter-diameter plug nozzle with a multispoke primary. Two multispoke primary nozzles, a 12-spoke and a 24-spoke, were tested and compared with an annular plug nozzle. The supersonic cruise configurations for both spoke primaries performed about the same, with a gross thrust coefficient of 0.974, a decrease of approximately 1.5 percent from the reference nozzle. The takeoff configuration for the 12-spoke primary had a gross thrust coefficient of 0.957, a decrease of 1.5 percent from the reference nozzle, and the 24-spoke primary had a gross thrust coefficient of 0.95.

17 Key Words (Suggested by Author(s))	18 Distribution Statement
Exhaust nozzle Nozzle performance Multispoke primary Propulsion	Unclassified - unlimited

19 Security Classif (of this report)	20 Security Classif (of this page)	21. No of Pages	22 Price*
Unclassified	Unclassified	39	$3.00

* For sale by the National Technical Information Service, Springfield, Virginia 22151

INTERNAL PERFORMANCE OF A 10° CONICAL PLUG NOZZLE WITH A MULTISPOKE PRIMARY AND TRANSLATING EXTERNAL SHROUD

by Donald L. Bresnahan

Lewis Research Center

SUMMARY

An experimental investigation was conducted in the Lewis Research Center's nozzle static test facility to determine the performance characteristics of a cold-flow, 21.59-centimeter-diameter plug nozzle with a multispoke primary and an overall design pressure ratio of 36. Two multispoke primary nozzles, a 12-spoke and a 24-spoke, were tested and compared with an annular plug nozzle. Various external shrouds were used to simulate takeoff and supersonic cruise configurations and also different methods of exposing the chutes to external flow.

At supersonic cruise with the chutes closed, the two multispoke primaries performed about the same, with a gross thrust coefficient of 0.974, down approximately 1.5 percent from that of the annular plug nozzle.

For takeoff, the configuration with the highest performance for the 12-spoke primary had a gross thrust coefficient of 0.957, a decrease of 1.5 percent from that of the reference nozzle. The 24-spoke primary had a gross thrust coefficient of 0.95.

INTRODUCTION

The Lewis Research Center is evaluating various nozzle concepts appropriate for supersonic cruise applications. These nozzles must operate efficiently over a wide range of flight conditions and engine power settings, which necessitates extensive geometric variations. Plug nozzles are receiving considerable emphasis because they may offer the potential of good aerodynamic performance together with a minimum of complexity and a consequent reduction in maintenance problems. Tests have been conducted (refs. 1 to 10) to optimize the performance of the low-angle plug nozzle, to determine the installation effects, and to determine the heat-transfer characteristics.

Another area of interest now is the noise level of the jet engines. During takeoff and climbout, the engines of supersonic-cruise aircraft produce considerable noise. A portion of this noise emanates from the high-velocity jets exiting from the exhaust nozzles. The noise produced by several nozzle types was recently evaluated at takeoff pressure ratios in a static test stand (ref. 11). The results showed the plug nozzle was the quietest. Static and flyover noise tests are also being conducted with a 12-spoke primary plug nozzle (63.5 cm diam) on a modified F-106B aircraft having underwing engine nacelles housing J85-GE-13 engines. These tests are to determine the noise suppression and performance statically and at flyovers at Mach 0.4 at 91.44 meters. Since the principal factor controlling this noise level is the jet velocity, reducing the jet velocity will result in lower noise levels. One method of accomplishing this would be to bring in low-energy air to mix with the exhaust gases by means of a spoked primary. This type nozzle will suffer some performance loss. The present investigation was conducted to determine what the performance penalty would be if a plug nozzle with a spoke primary were used for sound suppression. Primaries with 12 and 24 spokes were tested with a 10°-half-angle plug, cylindrical external shrouds of varying length to simulate translation, and an overall design pressure ratio of 36. The reference nozzle was the 14° conical-primary plug nozzle of reference 9. The tests were conducted in the Lewis Research Center's nozzle static test facility to determine the internal performance. Nozzle pressure ratio was varied up to 30, and secondary flow effects were also studied for corrected secondary flow rates to 10 percent. Dry air at room temperature was used for both primary and secondary flows.

SYMBOLS

D drag

d diameter

F thrust

l full plug length measured from nozzle throat

P total pressure

p static pressure

r radius

T total temperature

w weight flow rate

x axial distance measured from nozzle throat

y radial distance in plane of primary total-pressure rake

τ temperature ratio, T_s/T_p

ω weight flow ratio, w_s/w_p

Subscripts:

i ideal

max maximum

p primary

s secondary

0 ambient

7 nozzle inlet

APPARATUS AND INSTRUMENTATION

Installation in Static-Test Facility

A schematic view and photograph of the research hardware installation in the static-test facility is shown in figures 1 and 2. The nozzles were mounted on a section of pipe which was freely suspended by four flexure rods connected to the bedplate. Pressure forces acting on the nozzle and mounting pipe, both external and internal, were transmitted to a load cell which was used in measuring thrust.

The nozzle primary air flow was calculated from pressure and temperature measurements at the air-metering station (fig. 1) and an effective area determined by an ASME calibration nozzle. The secondary air flow was measured by means of a standard ASME flow-metering orifice in the external supply line.

The nozzle-inlet total pressure and temperature were measured at station 7, and ambient exhaust pressure was measured at station 0.

Nozzle Configurations

The nozzle configurations consisted of a 10°-half-angle plug with shrouds of varying lengths to simulate either takeoff or supersonic cruise configurations. The reference nozzle had a 14° conical primary with an annular throat. The basic model dimensions are shown in figure 3(a). Two external shrouds were tested - a retracted shroud ($x/d_{max} = -0.225$) to simulate a takeoff configuration and an extended shroud ($x/d_{max} = 0.674$) to simulate a supersonic cruise configuration.

The spoke nozzle is shown in figure 3(b), and details of the primary nozzles are shown in figure 3(c). For the takeoff configurations, four external shrouds were tested simulating various methods of opening the chute inlets to admit external air. These included two extended slotted shrouds (x/d_{max} = 0.449 and 0.741) shown in figure 3(d) and a fully retracted shroud (x/d_{max} = -0.906) to simulate different translations, and an extended shroud (x/d_{max} = 0.449) with floating doors as shown in figure 3(e). To simulate a supersonic cruise configuration, two extended solid shrouds (x/d_{max} = 0.449 and 0.741) were tested.

Photographs of the model hardware are presented in figure 4. Takeoff configurations with the fully-retracted shroud for the reference nozzle and the 12-spoke nozzle are shown in figures 4(a) and (b), respectively. The two multispoke primaries are shown in figure 4(c), and the solid shrouds tested with each are shown in figure 4(d). The slotted and floating door shrouds were tested with the 12-spoke primary only and are shown in figures 4(e) and (f), respectively.

Nozzle Instrumentation

The primary total pressure was measured by an area-weighted rake as shown in figure 5(a). The total-pressure distortion parameter ($(P_{7,max} - P_{7,min})/P_{7,av}$) varied from 0.018 for the reference nozzle to 0.021 for the two multispoke primary nozzles. Two thermocouples and two static-pressure orifices were located with the total-pressure rake. The secondary air total pressure was measured by four probes located as shown in figure 5(b). A row of static-pressure orifices was located on the plug at a meridian angle of 180° (fig. 5(c)). Static-pressure orifices were located on three primary nozzles as shown in figures 5(d) and (e). The spoke primaries had a total-pressure rake (fig. 5(f)) in one of the secondary chutes adjacent to the chute with the static-pressure orifices. The floating door shroud had static-pressure orifices located as shown in figure 5(g).

PROCEDURE

Pressure ratios were set by maintaining a constant nozzle-inlet pressure and varying the exhaust pressure. Each configuration was tested over a range of pressure ratios which were appropriate for the particular shroud extension ratio. For the takeoff configurations, corrected secondary weight-flow ratios of 0 and 4 percent were set for all nozzle pressure ratios tested. At a nozzle pressure ratio of 3.25, the corrected secondary weight-flow ratio was varied to 10 percent. For the supersonic cruise

configurations, the weight-flow ratio was set at 0 and 2 percent for all nozzle pressure ratios tested and at various weight-flow ratios to 10 percent at a pressure ratio of 27.5.

DATA REDUCTION

The nozzle primary airflow was calculated from pressure and temperature measurements at the air metering station in the necked-down section of the mounting pipe and an effective area determined by calibration with an ASME nozzle. The secondary airflow was measured by means of a standard ASME flow-metering orifice in the external supply line.

Actual jet thrust was calculated from load-cell measurements corrected for tare forces. The ideal jet thrust for each of the primary and secondary flows was calculated from the measured mass-flow rate expanded from their measured total pressures to p_0. Provision was made to equate the ideal thrust of the secondary flow to zero if the total pressure was less than p_0; however, this did not occur for the conditions tested.

The data are then presented as both nozzle gross thrust coefficient $((F - D)/F_{i,p})$ and nozzle efficiency, defined as the ratio of the gross thrust-minus-drag to the ideal gross thrust of both primary and secondary flows $((F - D)/F_{i,p} + F_{i,s})$.

The thrust system was calibrated by using a standard ASME sonic nozzle with a throat area nearly equal to the throat areas of the nozzles tested. The measured performance is compared with theoretical performance in figure 6. The results indicate approximately a ±1.0 percent maximum scatter in the gross thrust measurements. For the same set of data points, the standard deviation was 0.0044.

RESULTS AND DISCUSSION

The plug nozzle with multispoke primaries was tested to determine the performance penalty associated with this type of nozzle should it be used for noise suppression. Primaries with 12 and 24 spokes were tested, and their results are compared with the performance of an annular plug nozzle with a 14° conical primary.

A comparison of the gross thrust coefficient for the configurations tested is shown in figure 7. The takeoff configurations were compared at a nozzle pressure ratio of 3.25 and a nominal corrected secondary weight-flow ratio of 4 percent (fig. 7(a)). With the external shroud fully retracted, the performance of the 12-spoke primary decreased about 1.5 percent from that of the reference nozzle, and the performance of the 24-spoke primary dropped 2 percent. Some of this loss is due to the throats of the multispoke nozzles being located downstream on the plug, which results in lower forces on the plug surface and also additional internal skin friction losses. The 12-spoke primary was also

tested with two extended slotted shrouds (x/d_{max} = 0.449 and 0.741) to simulate translation and with one extended shroud with floating doors (x/d_{max} = 0.449). The performance of these configurations further decreased by approximately 5 to 10 percent, with the longest slotted shroud having the lowest gross thrust coefficient of 0.86. Pressure measurements along the secondary chutes and floating door showed increased drag for that configuration. With the shroud extended, there was insufficient tertiary air entering the slots and overexpansion losses resulted, as was indicated by reduced plug pressure distributions.

The supersonic cruise configurations were compared at a nozzle pressure ratio of 27.5 and a nominal secondary weight-flow ratio of 2 percent (fig. 7(b)). Two external shrouds were tested with each of the spoke primaries and, in general, their performance was the same, with a decrease of about 1.5 percent from that of the reference nozzle. This was due to a net loss in primary and plug thrust and additional internal skin friction losses from the spoke primaries.

Nozzle efficiencies for the takeoff and supersonic cruise configurations are presented in figure 8.

To minimize the drag induced by the internal base formed by the primary nozzles and for cooling purposes, some secondary flow is required. As indicated in the following sketch, choking of the secondary flow can occur at two locations. With the jet attached to

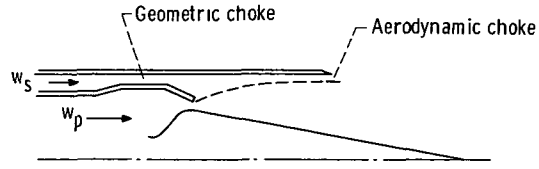

the secondary shroud, an aerodynamic choke point for the secondary flow would exist near the attachment point. If the secondary flow rate is increased sufficiently, a second choke point can exist at the minimum geometric secondary flow area upstream of the boattail. Under these conditions, the secondary flow can become supersonic at all stations downstream of the geometric choke point. If the aerodynamic choke point is eliminated either by operating the nozzle at such low primary pressure ratios that the jet is detached from the secondary shroud or by translating the shroud upstream so that jet attachment cannot occur, then only geometric choking of the secondary flow can occur.

A comparison of the pumping characteristics of the multispoke nozzles with that of the annular nozzle is shown in figure 9. The takeoff configurations with the shroud retracted and a nominal corrected secondary weight-flow ratio of 4 percent (fig. 9(a)) shows geometric choking for the two multispoke primaries at the higher nozzle pressure ratios and the reference nozzle is approaching a choked condition. The three nozzles choke at different levels of P_s/P_7 because of the differences in secondary flow areas. The reference nozzle has the largest secondary flow area and, therefore, the lowest secondary total pressure ratio. The spoke nozzles having a smaller secondary passage require a larger total pressure to pass the same secondary flow, hence a higher secondary total pressure ratio.

For the supersonic cruise configurations (fig. 9(b)) and a nominal secondary weight-flow ratio of 2 percent, the secondary total pressure ratio was independent of primary nozzle pressure ratio over the range investigated. This indicates that the primary jet was attached to the extended secondary shroud and aerodynamic choking existed. With these nozzles having nearly the same internal expansion and operating under similar conditions, the aerodynamic choking areas are apparently the same as indicated by the nozzles having the same secondary total pressure ratios.

The pumping characteristics for the four shrouds tested with the 12-spoke primary for takeoff are given in figure 10. Again there is geometric choking of the secondary flow at the higher nozzle pressure ratios. For the retracted shroud ($x/d_{max} = -0.906$) and the two extended slotted shrouds ($x/d_{max} = 0.449$ and 0.741), the minimum secondary flow area is the same; therefore, the pumping curve is the same. With the doors open on the floating-door shroud, the minimum secondary area is reduced near the hinge point, and a higher total secondary pressure is required for the same weight flow. Hence, the pumping curve is displaced upward.

Nozzle performance and pumping curves for all the takeoff configurations tested are presented in figure 11. Data are shown for corrected secondary weight-flow ratios of 0 and 4 percent over the range of nozzle pressure ratios tested to show the effect of nozzle pressure ratio. For the retracted-shroud configurations, the nozzle gross thrust coefficient and efficiency peaked near the takeoff pressure ratio of 3.25. As the shroud was extended, overexpansion occurred, which shifted the peak to higher pressure ratios. There was insufficient tertiary air entering the slots to prevent this overexpansion.

The effect of corrected secondary weight-flow ratio for the same parameters and nozzle configurations is shown in figure 12 for the takeoff nozzle pressure ratio of 3.25. In general, secondary flow did not improve nozzle efficiency. However, with the floating doors there was a peak at 2 percent.

Nozzle performance and pumping characteristics for the supersonic-cruise configurations are presented in figure 13. Data are shown for corrected secondary weight-flow ratios of 0 and 2 percent over the range of nozzle pressure ratios tested. From the

pumping curves it can be seen that the secondary total pressure ratio was independent of the primary nozzle pressure ratio, which indicates that the secondary flow is choked.

The effect of secondary flow on the nozzle performance and pumping characteristics is shown in figure 14 for the supersonic-cruise configurations at a nominal nozzle pressure ratio of 27.5. From the nozzle efficiency and pumping curves it can be seen that the efficiency increases with corresponding increases in secondary flow until the secondary flow is choked, after which the efficiency decreases. This choking occurred near 4 percent for the multispoke nozzles.

SUMMARY OF RESULTS

An experimental investigation was conducted to determine the internal performance of a 10° conical plug nozzle with a multispoke primary and translating external shroud. Two primary nozzles were tested - one with 12 spokes and the other with 24 spokes. The performance of these two nozzles was then compared with that of a reference nozzle which was a 10° conical plug nozzle with a 14° conical primary. The following general trends were indicated:

1. At supersonic cruise with the chutes closed, both multispoke primaries performed about the same, with a gross thrust coefficient of 0.974, down approximately 1.5 percent from that of the reference nozzle.

2. The 12-spoke primary with the fully retracted shroud had the best takeoff performance, with a gross thrust coefficient of 0.957, a decrease of 1.5 percent from that of the reference nozzle. The shorter slotted shroud ($x/d_{max} = 0.449$) had a gross thrust coefficient of 0.91, and the longer one ($x/d_{max} = 0.741$) had the lowest performance at 0.86. The floating-door shroud ($x/d_{max} = 0.449$) had a gross thrust coefficient of 0.87.

3. The 24-spoke primary with the fully retracted shroud had a gross thrust coefficient of 0.95, down more than 2 percent from that of the reference nozzle.

Lewis Research Center,
National Aeronautics and Space Administration,
Cleveland, Ohio, April 17, 1972,
764-74.

REFERENCES

1. Bresnahan, Donald L.; and Johns, Albert L.: Cold Flow Investigation of a Low Angle Turbojet Plug Nozzle With Fixed Throat and Translating Shroud at Mach Numbers From 0 to 2.0. NASA TM X-1619, 1968.

2. Wasko, Robert A.; and Harrington, Douglas E.: Performance of a Collapsible Plug Nozzle Having Either Two-Position Cylindrical or Variable Angle Floating Shrouds at Mach Numbers From 0 to 2.0. NASA TM X-1657, 1968.

3. Bresnahan, Donald L.: Experimental Investigation of a 10^{o} Conical Turbojet Plug Nozzle with Iris Primary and Translating Shroud at Mach Numbers From 0 to 2.0. NASA TM X-1709, 1968.

4. Bresnahan, Donald L.: Experimental Investigation of a 10^{o} Conical Turbojet Plug Nozzle with Translating Primary and Secondary Shrouds at Mach Numbers From 0 to 2.0. NASA TM X-1777, 1969.

5. Johns, Albert L.: Quiescent-Air Performance of a Truncated Turbojet Plug Nozzle with Shroud and Plug Base Flows From a Common Source. NASA TM X-1807, 1969.

6. Huntley, Sidney C.; and Samanich, Nick E.: Performance of a 10^{o} Conical Plug Nozzle Using a Turbojet Gas Generator. NASA TM X-52570, 1969.

7. Jeracki, Robert J.; and Chenoweth, Francis C.: Coolant Flow Effects on the Performance of a Conical Plug Nozzle at Mach Numbers From 0 to 2.0. NASA TM X-2076, 1970.

8. Chenoweth, Francis C.; and Lieberman, Arthur: Experimental Investigation of Heat-Transfer Characteristics of a Film-Cooled Plug Nozzle with Translating Shroud. NASA TN D-6160, 1971.

9. Harrington, Douglas E.: Performance of a 10^{o} Conical Plug Nozzle with Various Primary Flap and Nacelle Configurations at Mach Numbers From 0 to 1.97. NASA TM X-2086, 1970.

10. Samanich, Nick E.; and Chamberlin, Roger: Flight Investigation of Installation Effects on a Plug Nozzle Installed on an Underwing Nacelle. NASA TM X-2295, 1971.

11. Darchuk, George V.; and Balombin, Joseph R.: Noise Evaluation of Four Exhaust Nozzles for Afterburning Turbojet Engine. NASA TM X-2014, 1970.

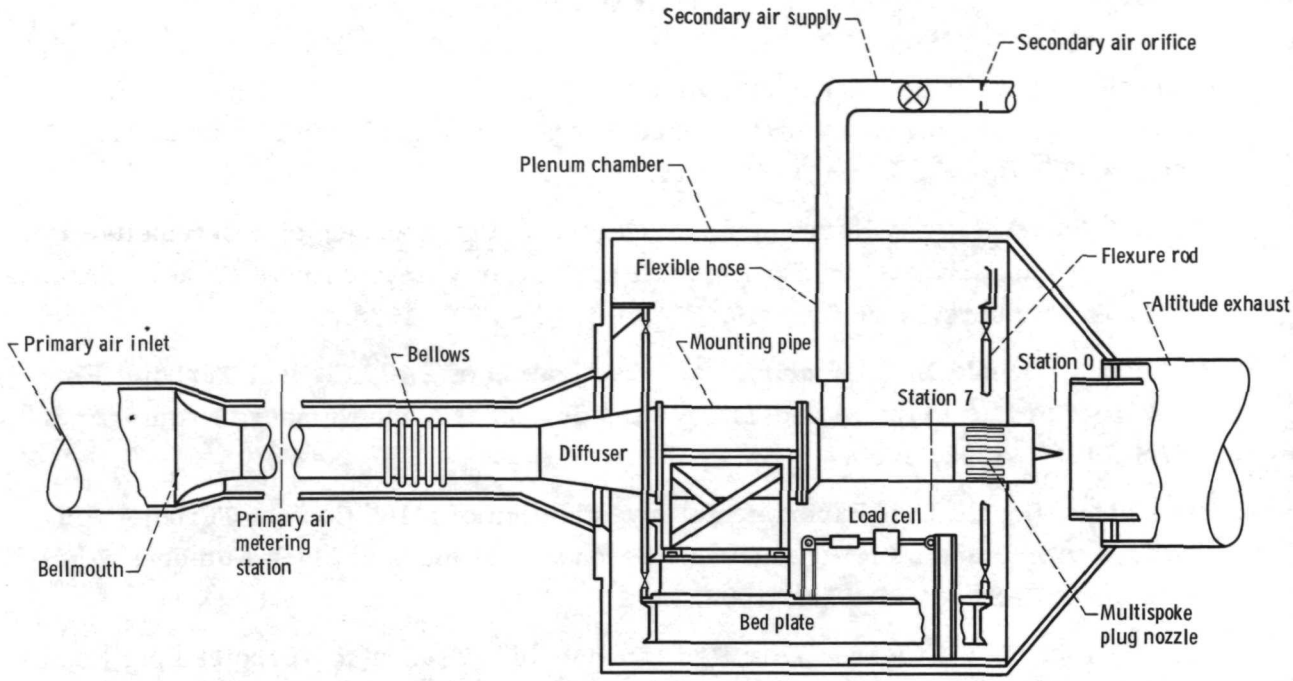

Figure 1. - Schematic view of static test stand.

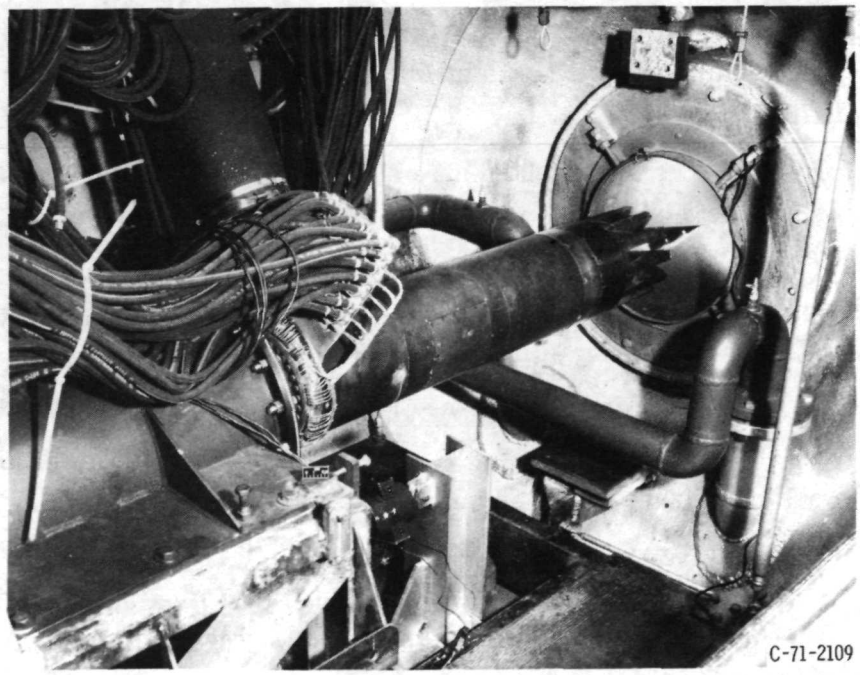

Figure 2. - Installation of nozzle in static test stand.

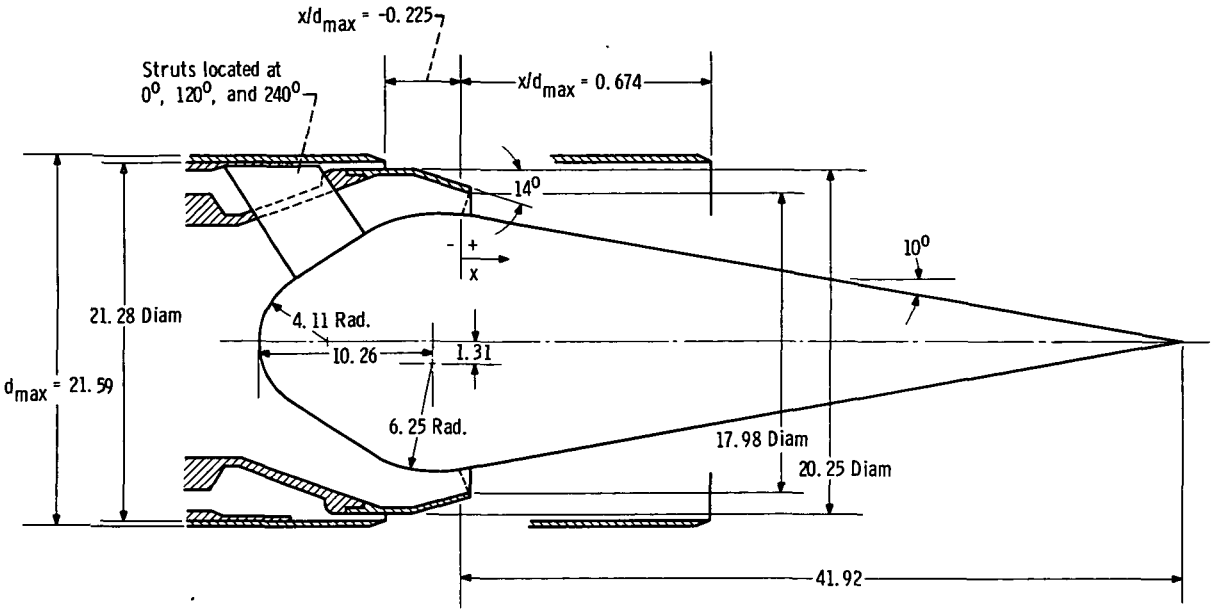

(a) Reference nozzle.

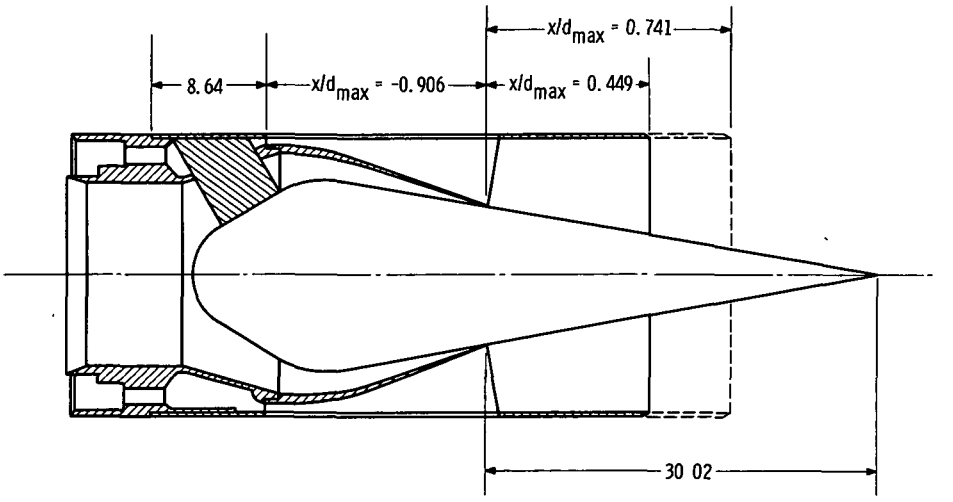

(b) Spoke nozzle.

Figure 3. - Model dimensions and geometric variables. (All dimensions in centimeters unless otherwise noted.)

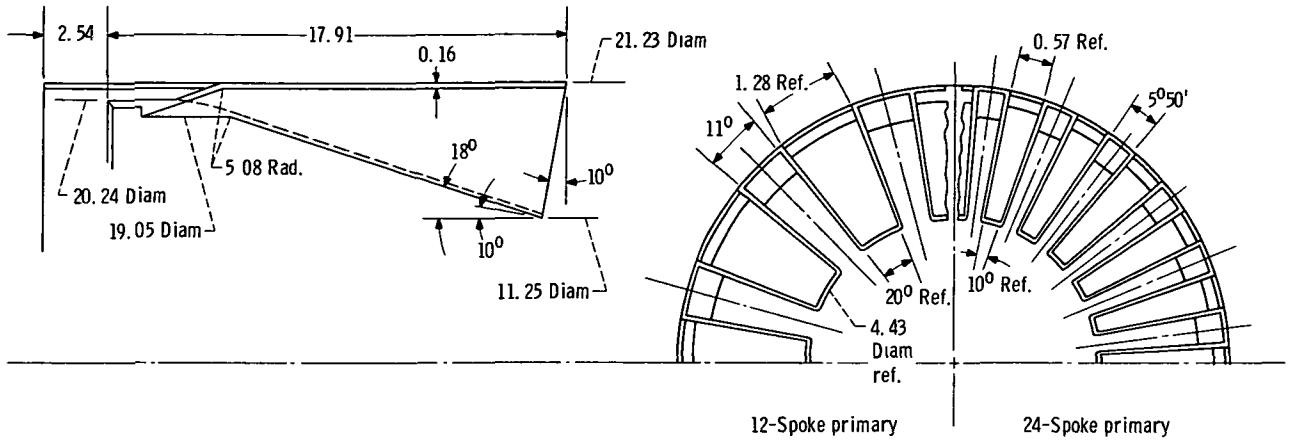

(c) Spoke primaries.

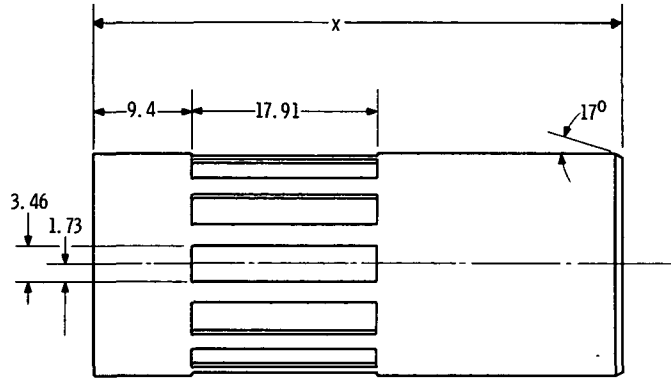

x	x/d_{max}
37.85	0.449
44 20	.741

(d) Slotted shroud.

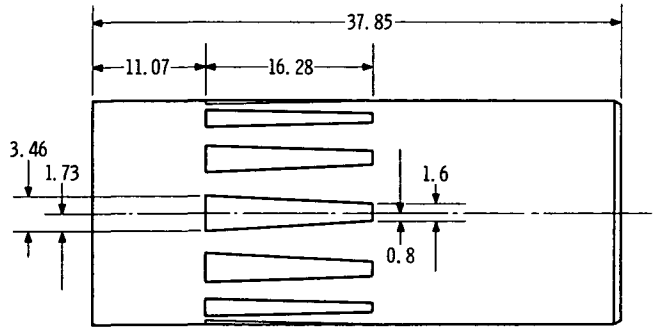

(e) Floating-door shroud.

Figure 3. - Concluded.

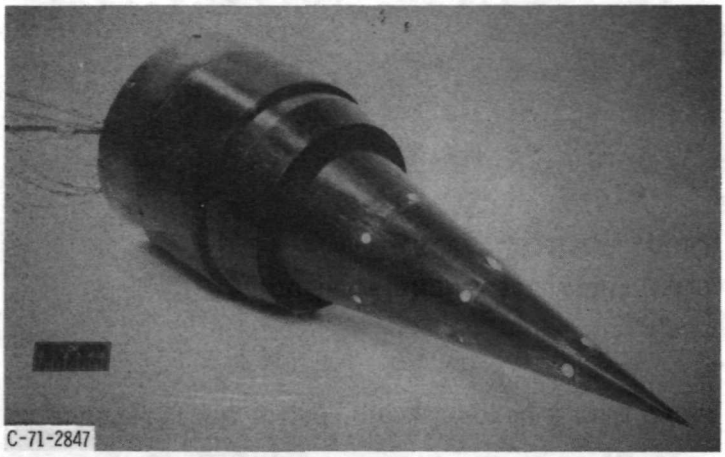

(a) Reference-nozzle takeoff configuration.

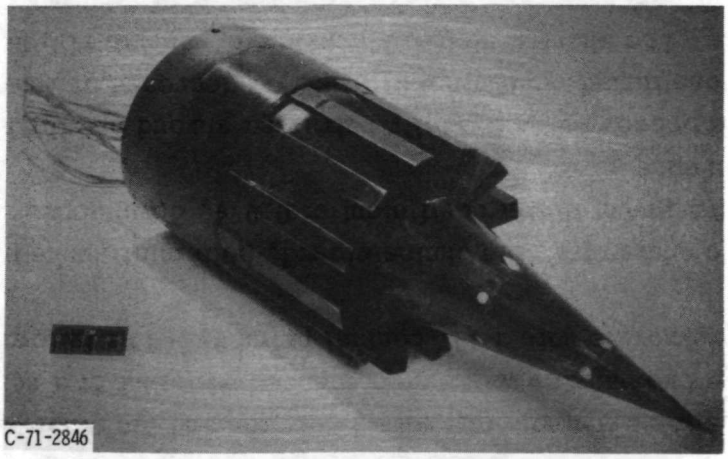

(b) Spoke-nozzle takeoff configuration.

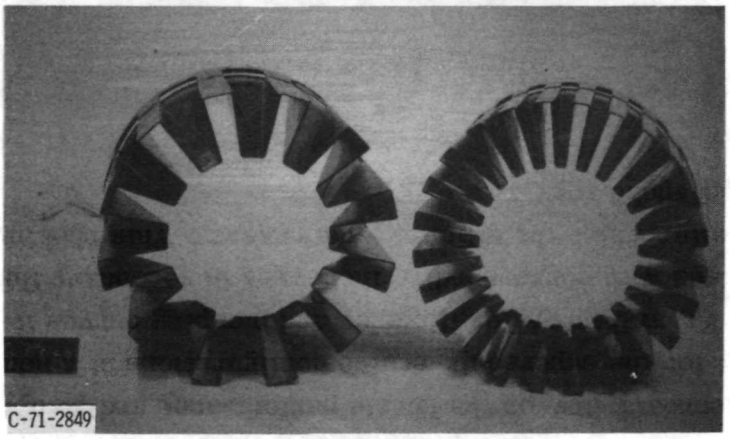

(c) Spoke primaries.

Figure 4. - Model hardware.

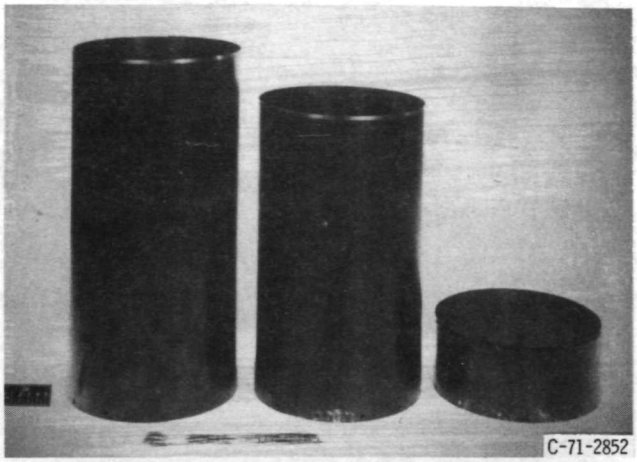

(d) Solid shrouds.

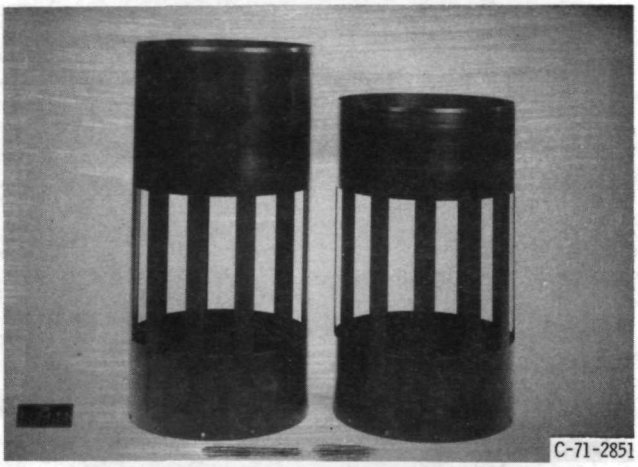

(e) Slotted shrouds.

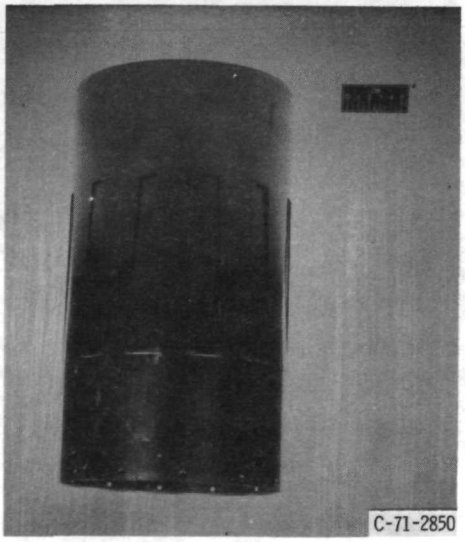

(f) Floating-door shroud.

Figure 4. - Concluded.

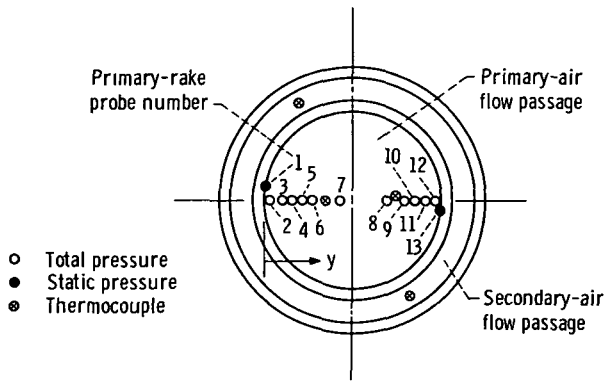

Primary-rake probe number	Distance, y
1	0
2	.16
3	.91
4	1.75
5	2.74
6	3.98
7	5.99
8	10.44
9	11.92
10	13.01
11	13.92
12	14.71
13	15.27

(a) Station-7 instrumentation.

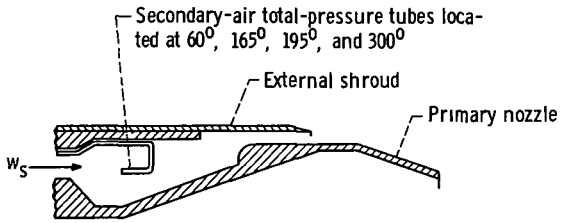

(b) Secondary-air total-pressure instrumentation.

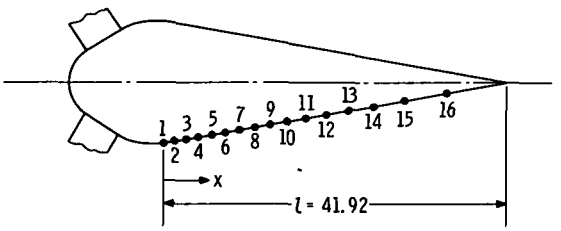

(c) Plug static-pressure orifice locations.

Orifice	x	x/l
1	0	0
2	.84	.02
3	2.31	.06
4	3.84	.09
5	5.44	.13
6	7.09	.17
7	8.84	.21
8	10.69	.25
9	12.65	.30
10	14.76	.35
11	17.02	.41
12	19.53	.47
13	22.23	.53
14	25.30	.60
15	29.06	.69
16	34.44	.82

Figure 5. - Model instrumentation. (All dimensions in centimeters unless otherwise noted.)

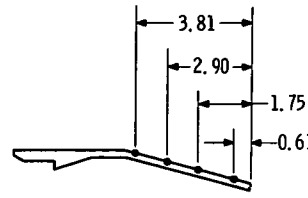

(d) Reference-primary static-pressure orifice locations.

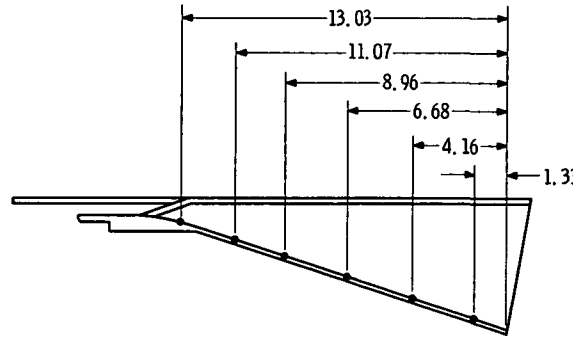

(e) Spoke-primary static-pressure orifice locations.

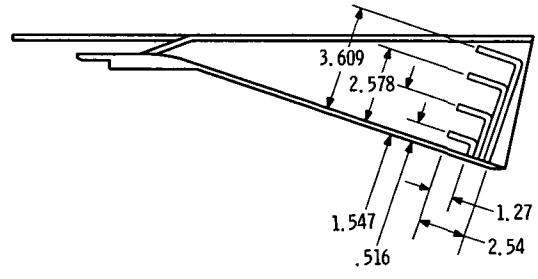

(f) Spoke-primary chute total-pressure rake.

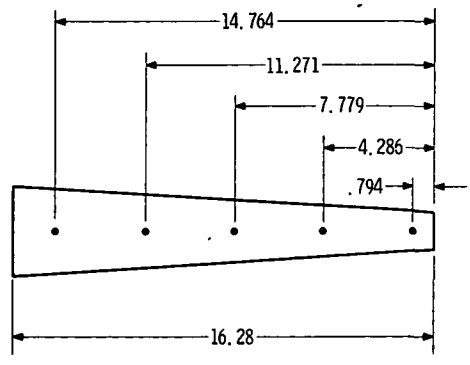

(g) Floating-door static-pressure orifice locations.

Figure 5. - Concluded.

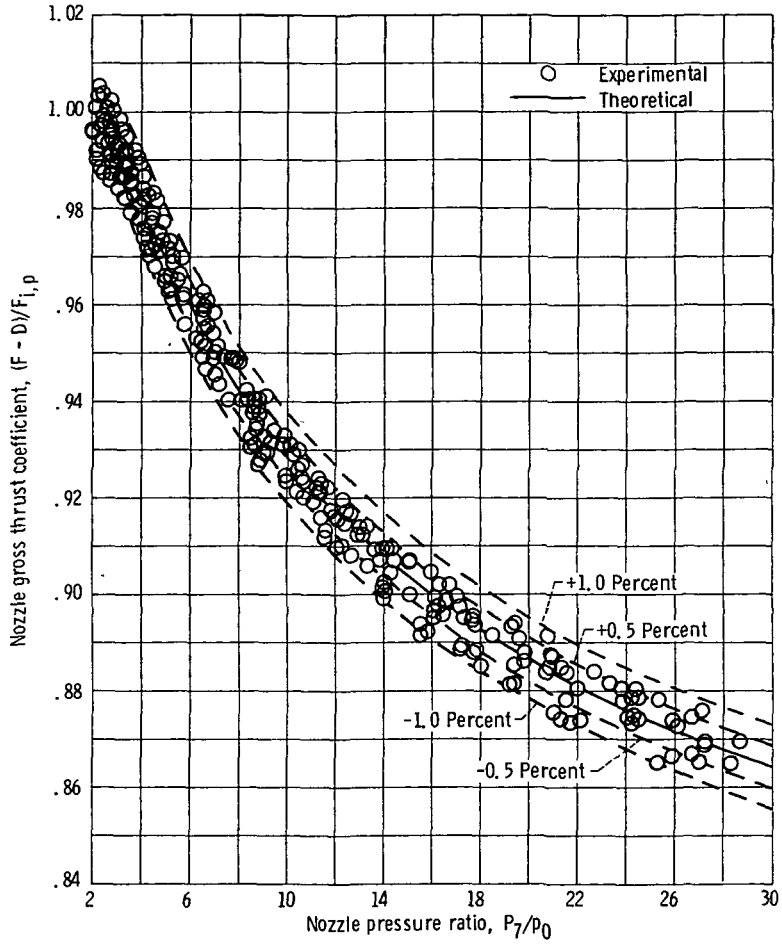

Figure 6. - Internal performance of ASME calibration nozzle.

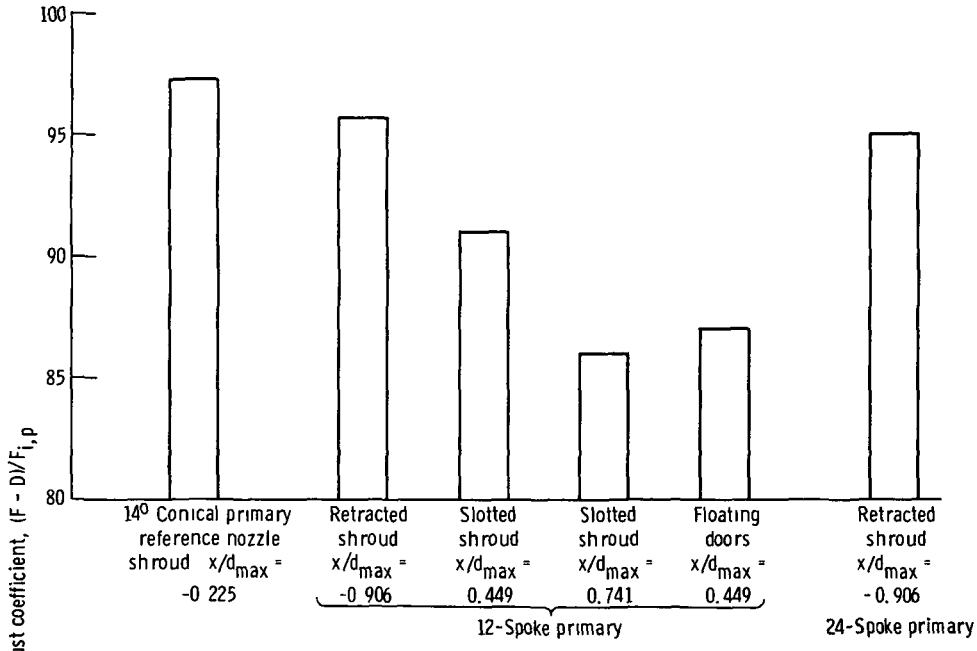

(a) Takeoff configurations. Nozzle pressure ratio, 3.25; corrected secondary weight-flow ratio, 0.04.

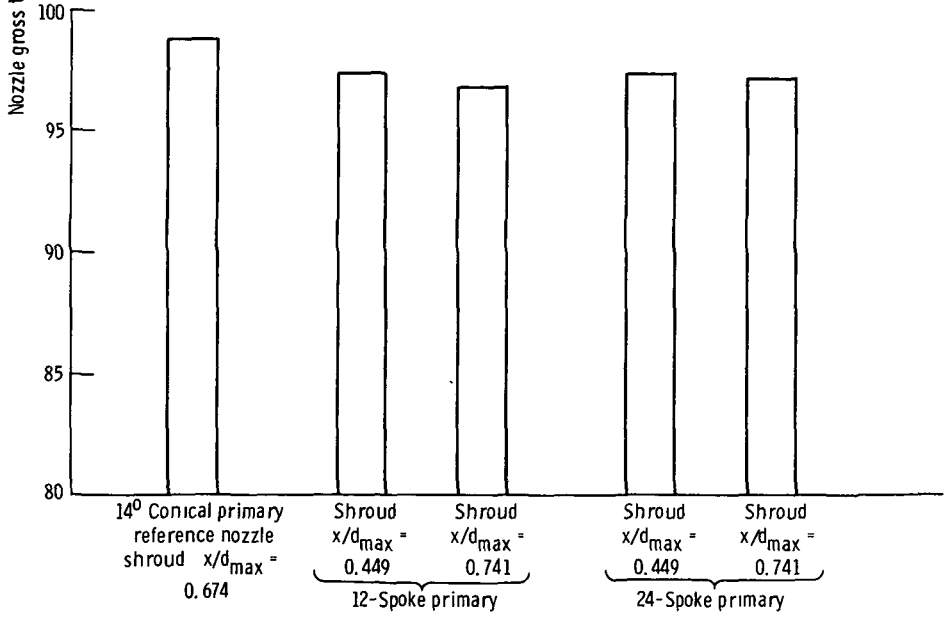

(b) Supersonic-cruise configurations. Nozzle pressure ratio, 27.5; corrected secondary weight-flow ratio, 0.02.

Figure 7. - Comparison of multispoke plug nozzle gross thrust coefficient with that of an annular plug nozzle.

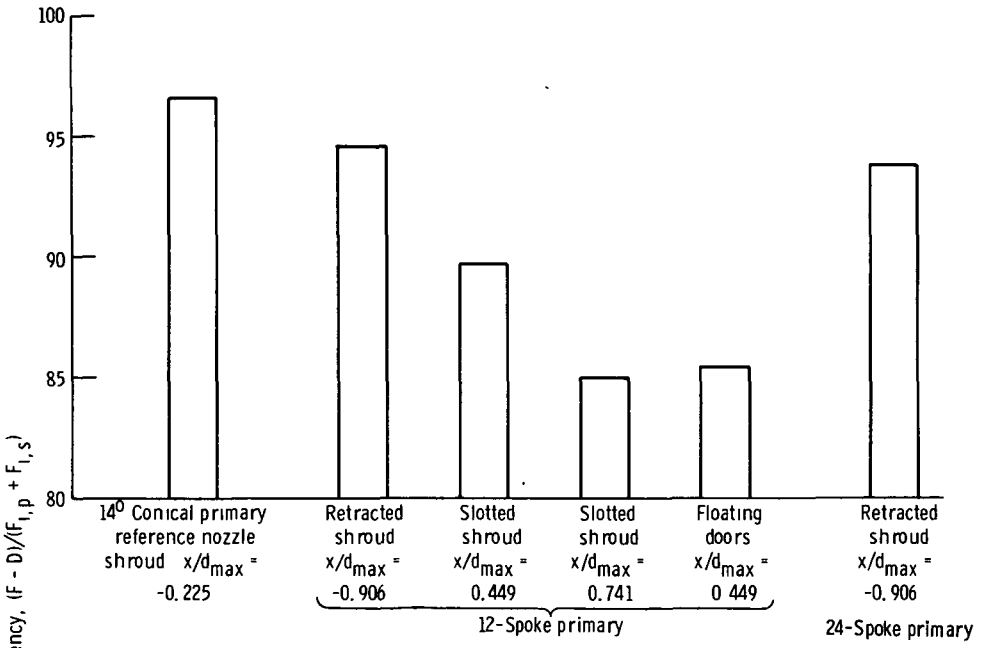

(a) Takeoff configurations. Nozzle pressure ratio, 3.25; corrected secondary weight-flow ratio, 0.04.

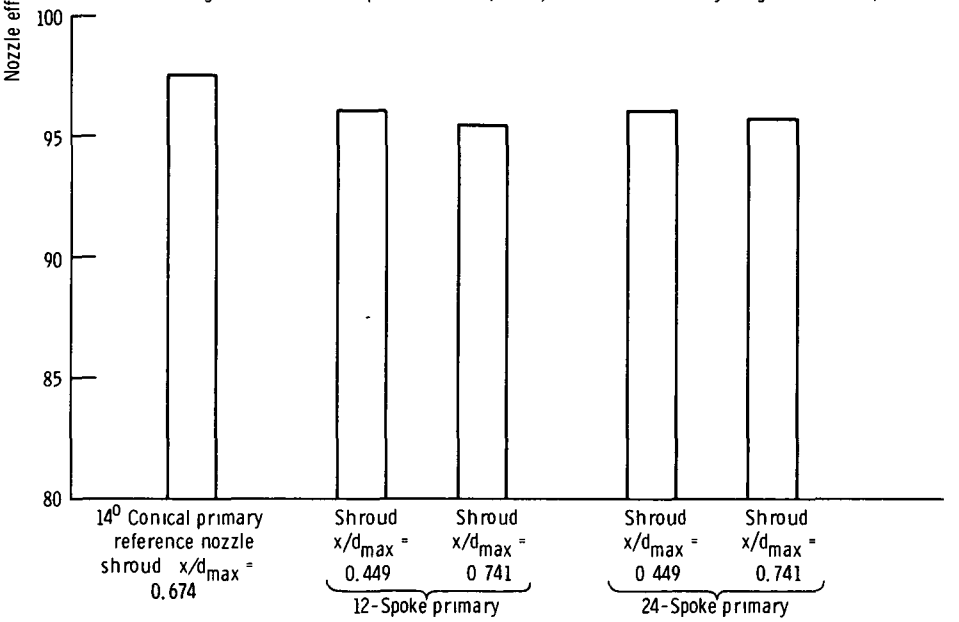

(b) Supersonic-cruise configurations Nozzle pressure ratio, 27 5, corrected secondary weight-flow ratio, 0.02.

Figure 8. - Comparison of multispoke plug nozzle efficiency with that of an annular plug nozzle.

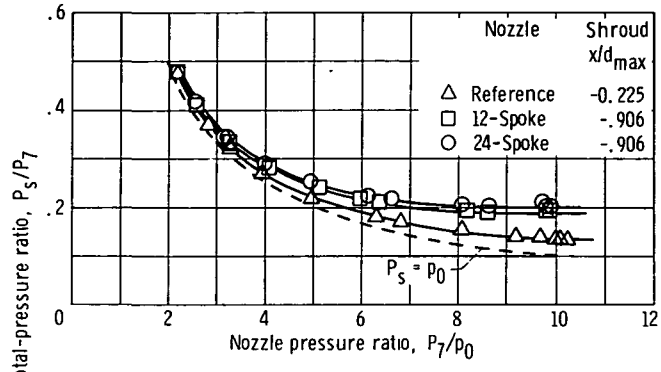

(a) Takeoff configurations; corrected secondary weight-flow ratio, 0 04.

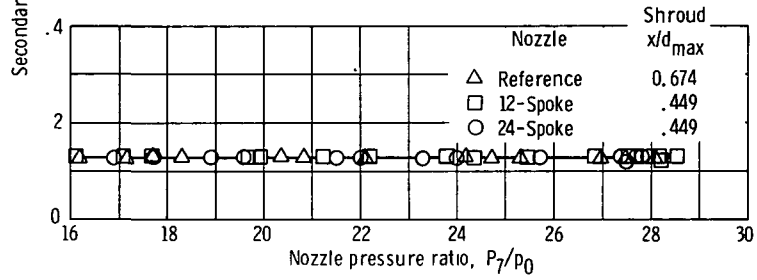

(b) Supersonic-cruise configurations, corrected secondary weight-flow ratio, 0 02.

Figure 9 - Comparison of the pumping characteristics of multispoke nozzles with that of an annular nozzle.

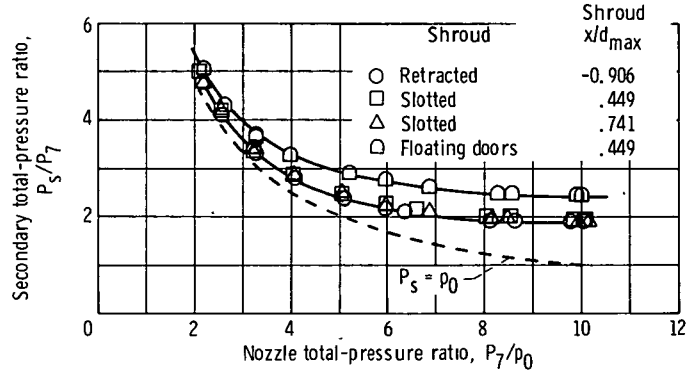

Figure 10. - Comparison of pumping characteristics of the takeoff shroud configurations for the 12-spoke primary nozzle. Corrected secondary weight-flow ratio, 0.04.

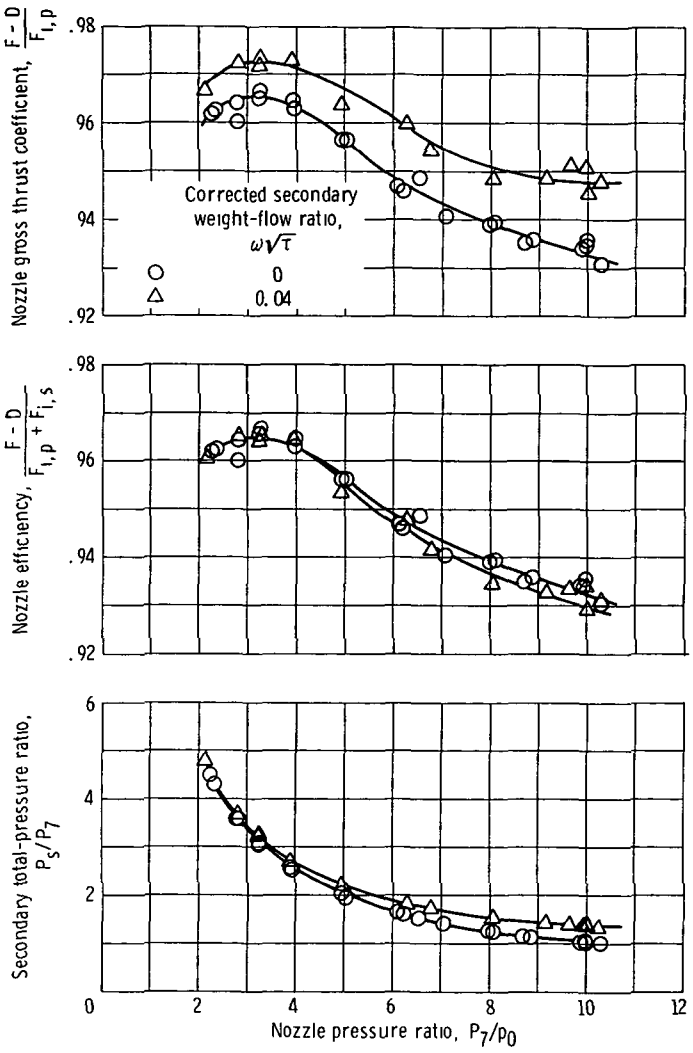

(a) Reference nozzle; shroud $x/d_{max} = -0.225$.

Figure 11 - Nozzle performance and pumping characteristics as functions of nozzle pressure ratio for takeoff configurations.

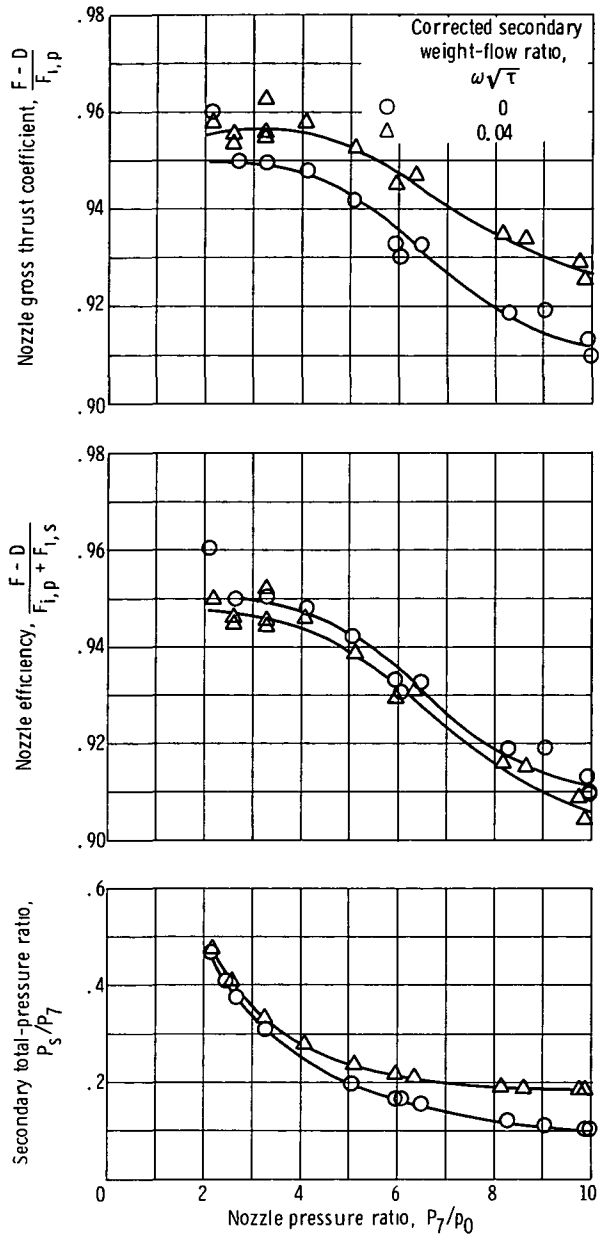

(b) 12-Spoke nozzle; shroud $x/d_{max} = -0.906$.

Figure 11 - Continued.

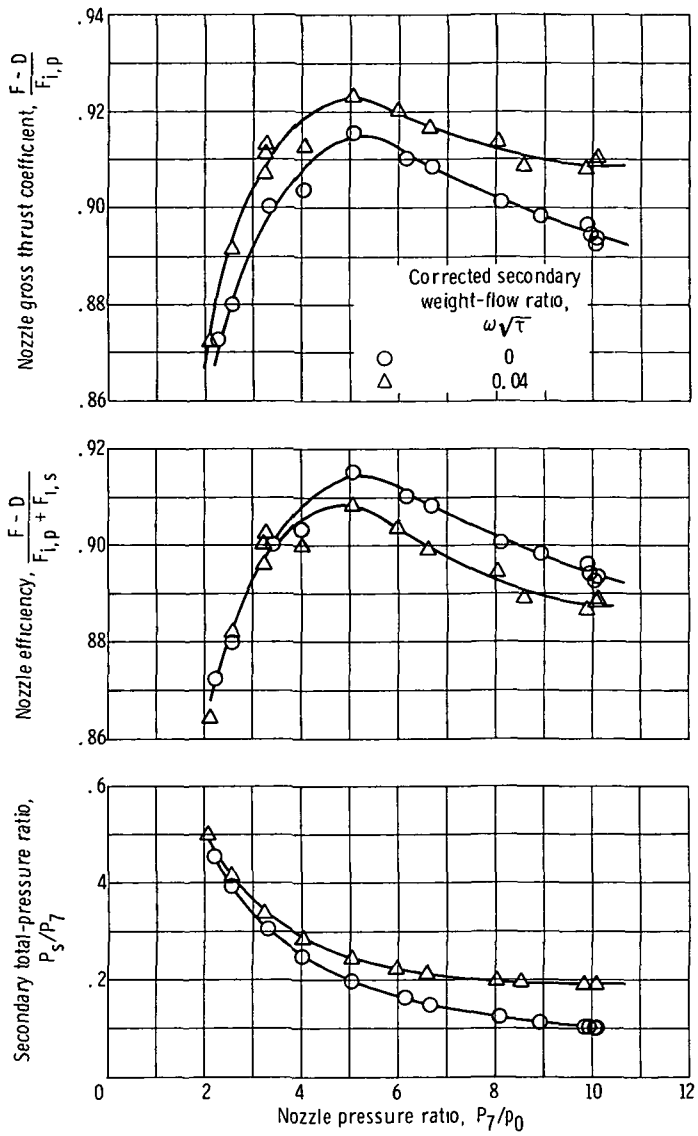

(c) 12-Spoke nozzle; slotted shroud $x/d_{max} = 0.449$

Figure 11 - Continued.

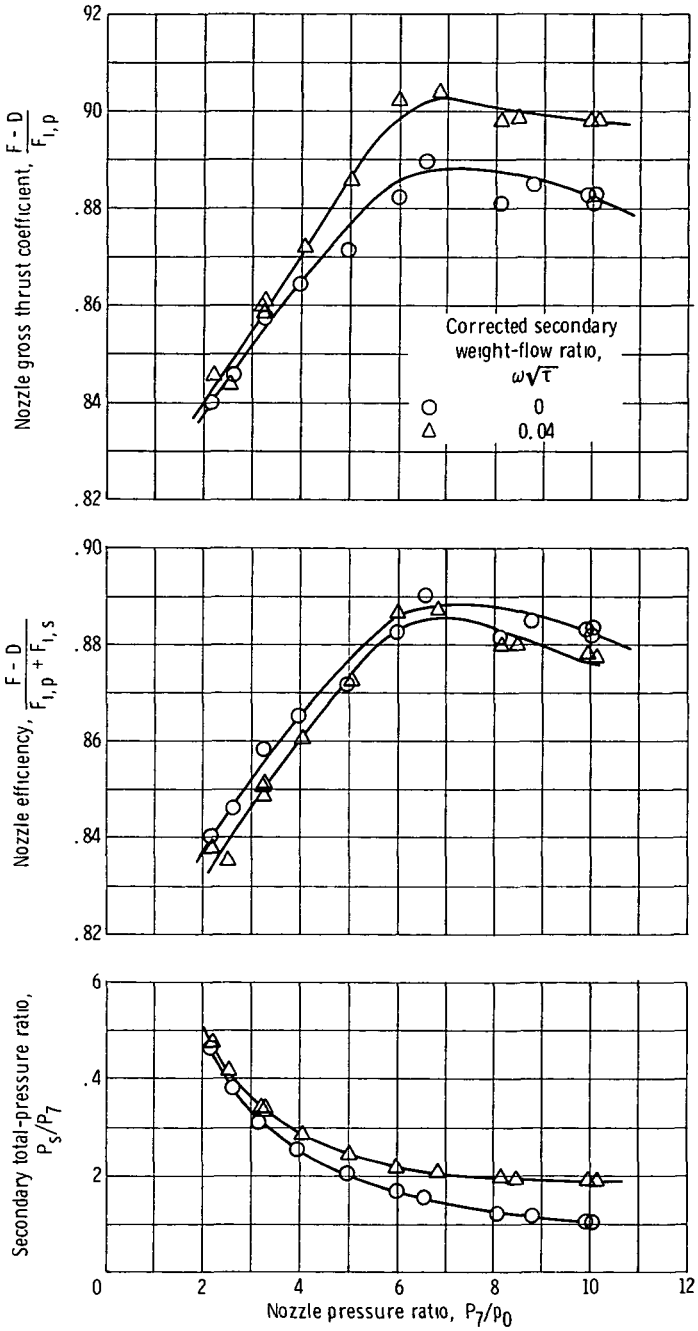

(d) 12-Spoke nozzle; slotted shroud $x/d_{max} = 0.741$.

Figure 11. - Continued.

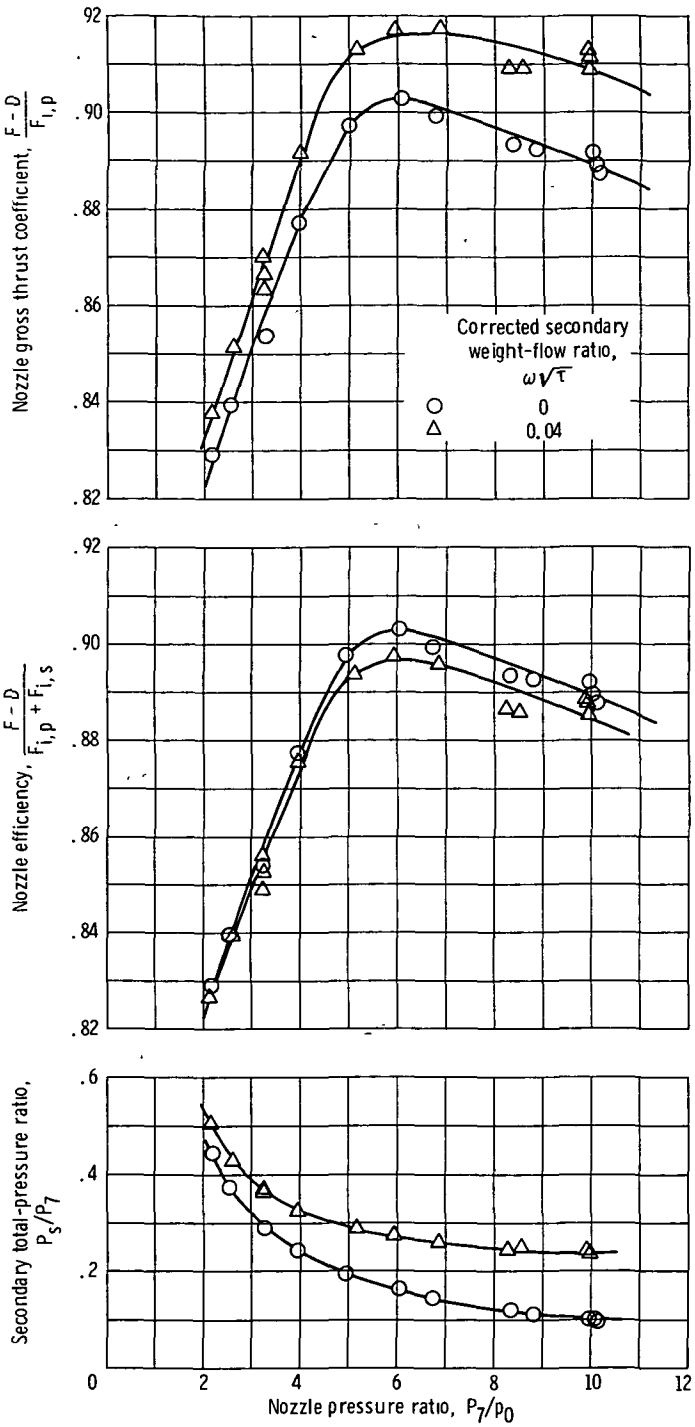

(e) 12-Spoke nozzle; floating-door shroud $x/d_{max} = 0.449$.

Figure 11. - Continued.

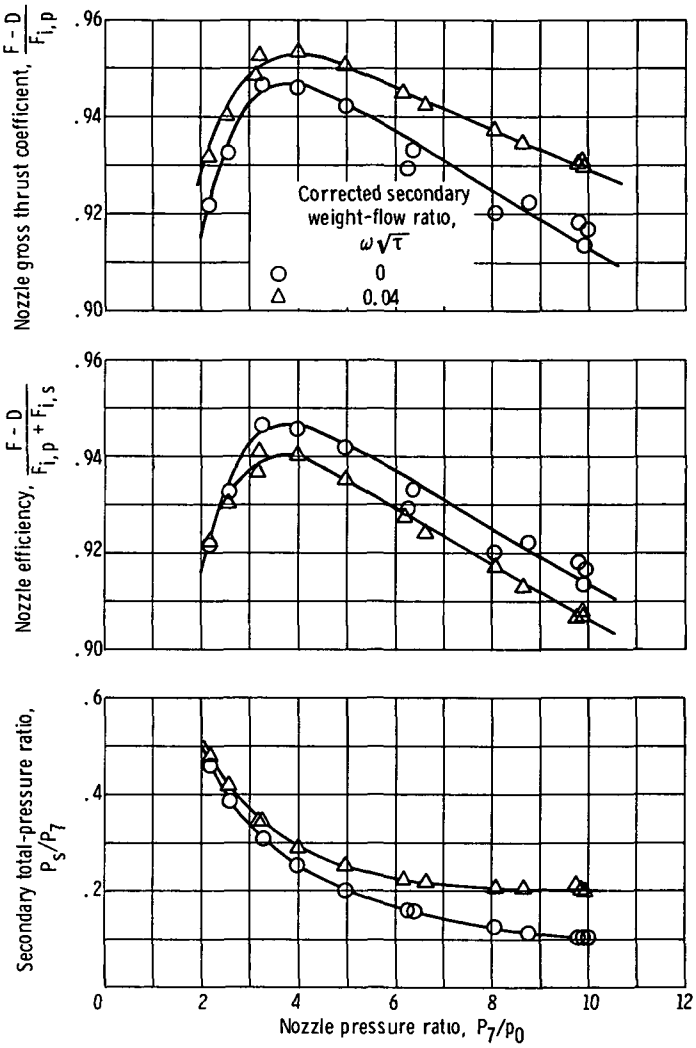

(f) 24-Spoke nozzle; shroud $x/d_{max} = -0.906$.

Figure 11. - Concluded.

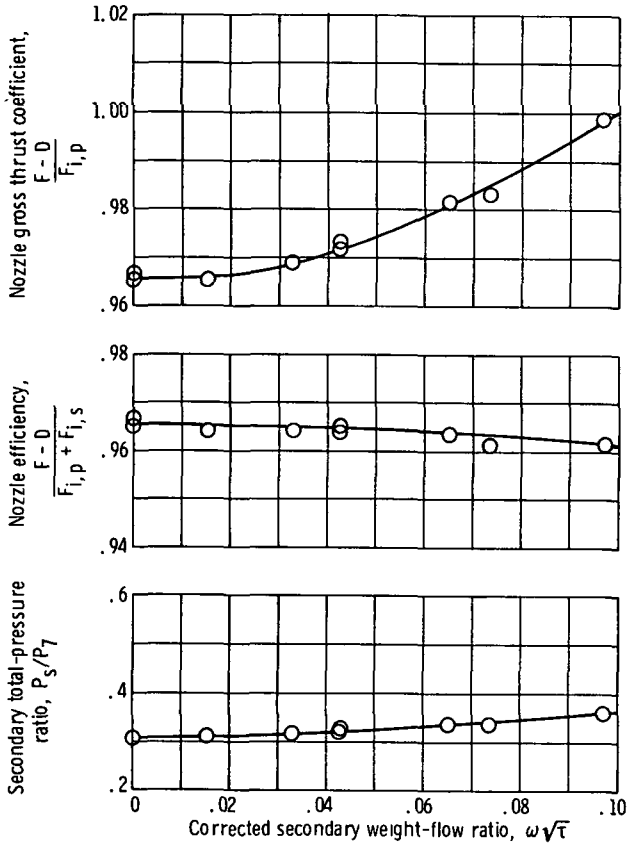

(a) Reference nozzle; shroud $x/d_{max} = -0.225$.

Figure 12. - Nozzle performance and pumping characteristics as functions of corrected secondary weight-flow ratio for takeoff configurations. Nozzle pressure ratio, 3.25.

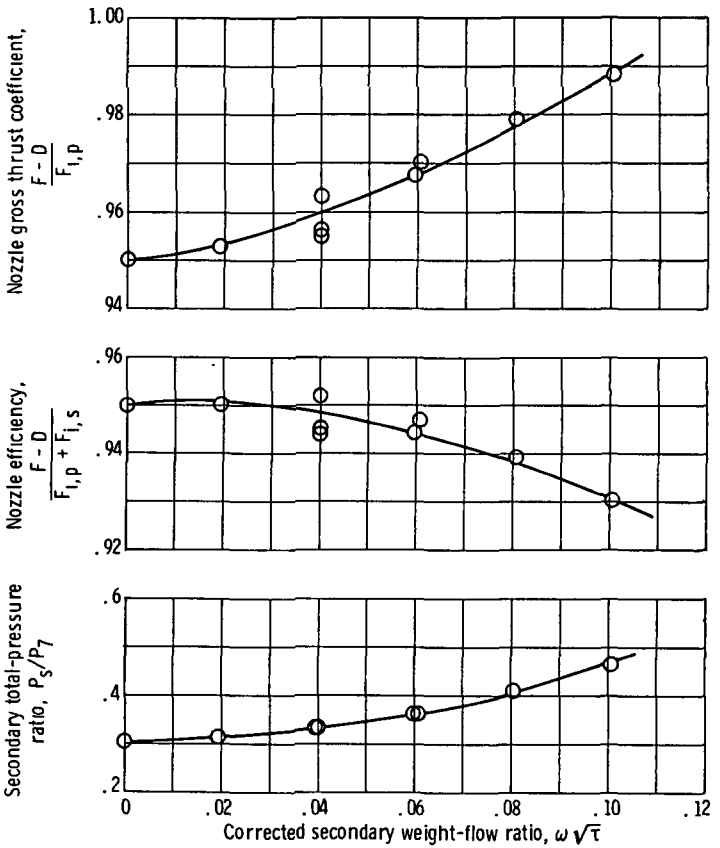

(b) 12-Spoke nozzle, shroud $x/d_{max} = -0.906$.

Figure 12. - Continued.

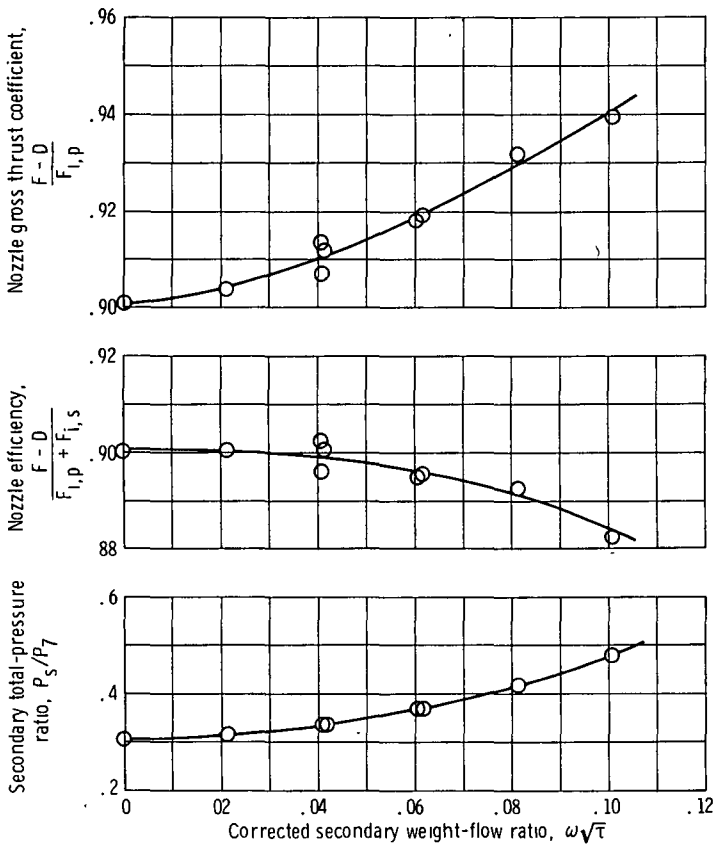

(c) 12-Spoke nozzle, slotted shroud $x/d_{max} = 0.449$.

Figure 12. - Continued

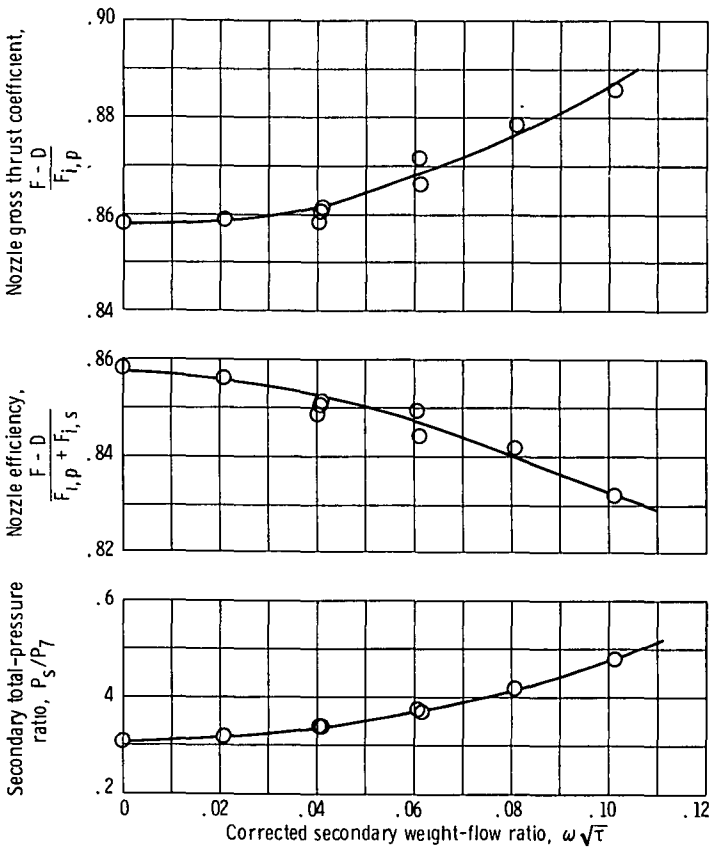

(d) 12-Spoke nozzle; slotted shroud $x/d_{max} = 0.741$.

Figure 12. - Continued.

(f) 24-Spoke nozzle; shroud $x/d_{max} = -0.906$.

Figure 12. - Concluded.

(e) 12-Spoke nozzle, floating-door shroud $x/d_{max} = 0.449$.

Figure 12. - Continued.

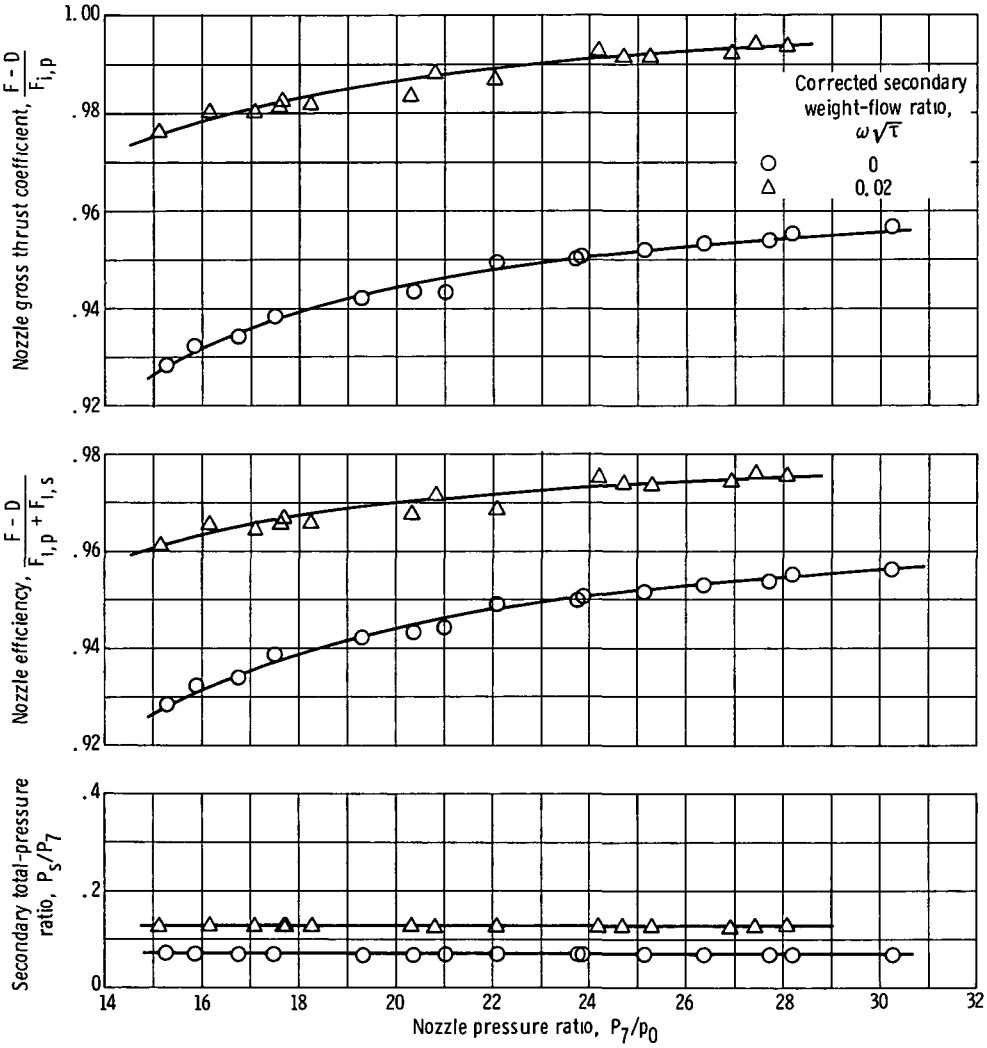

(a) Reference nozzle; shroud $x/d_{max} = 0.674$.

Figure 13. - Nozzle performance and pumping characteristics as functions of nozzle pressure ratio for supersonic cruise configurations.

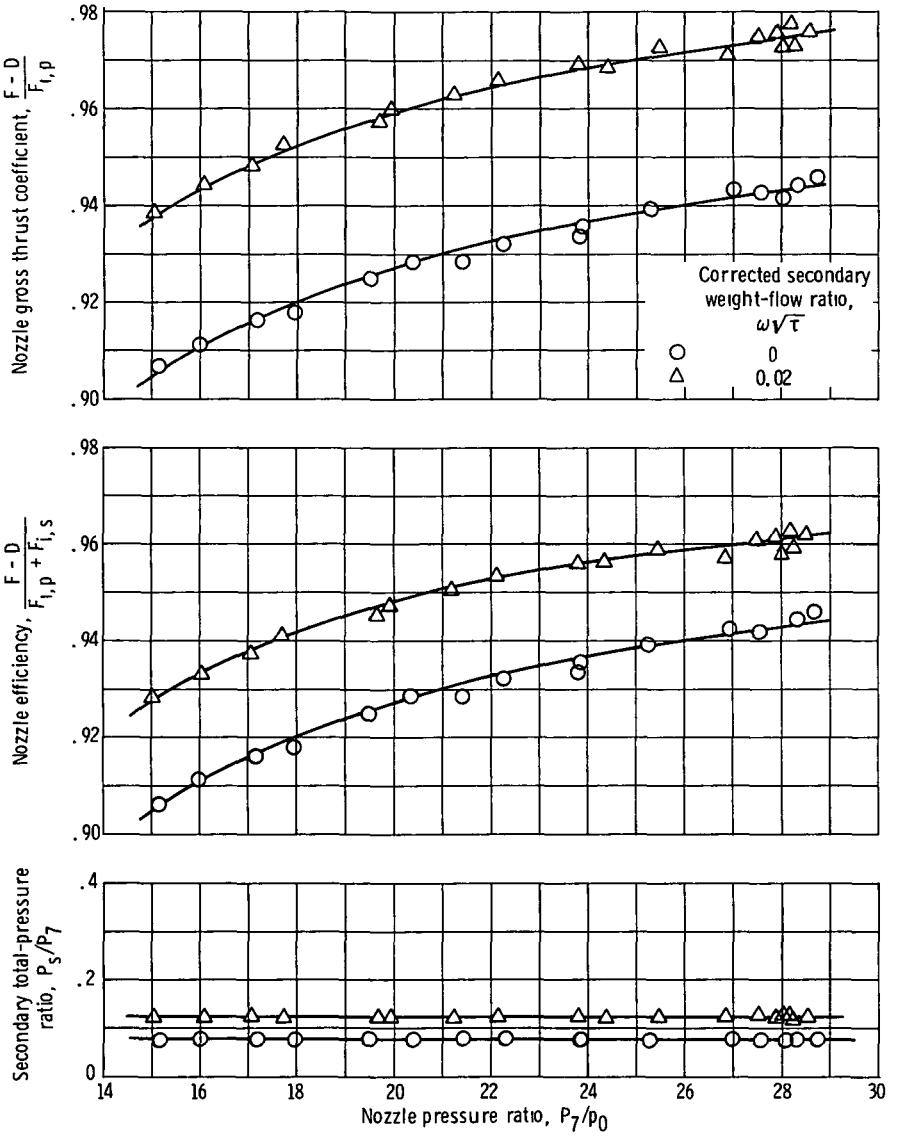

(b) 12-Spoke nozzle; shroud $x/d_{max} = 0.449$.

Figure 13. - Continued.

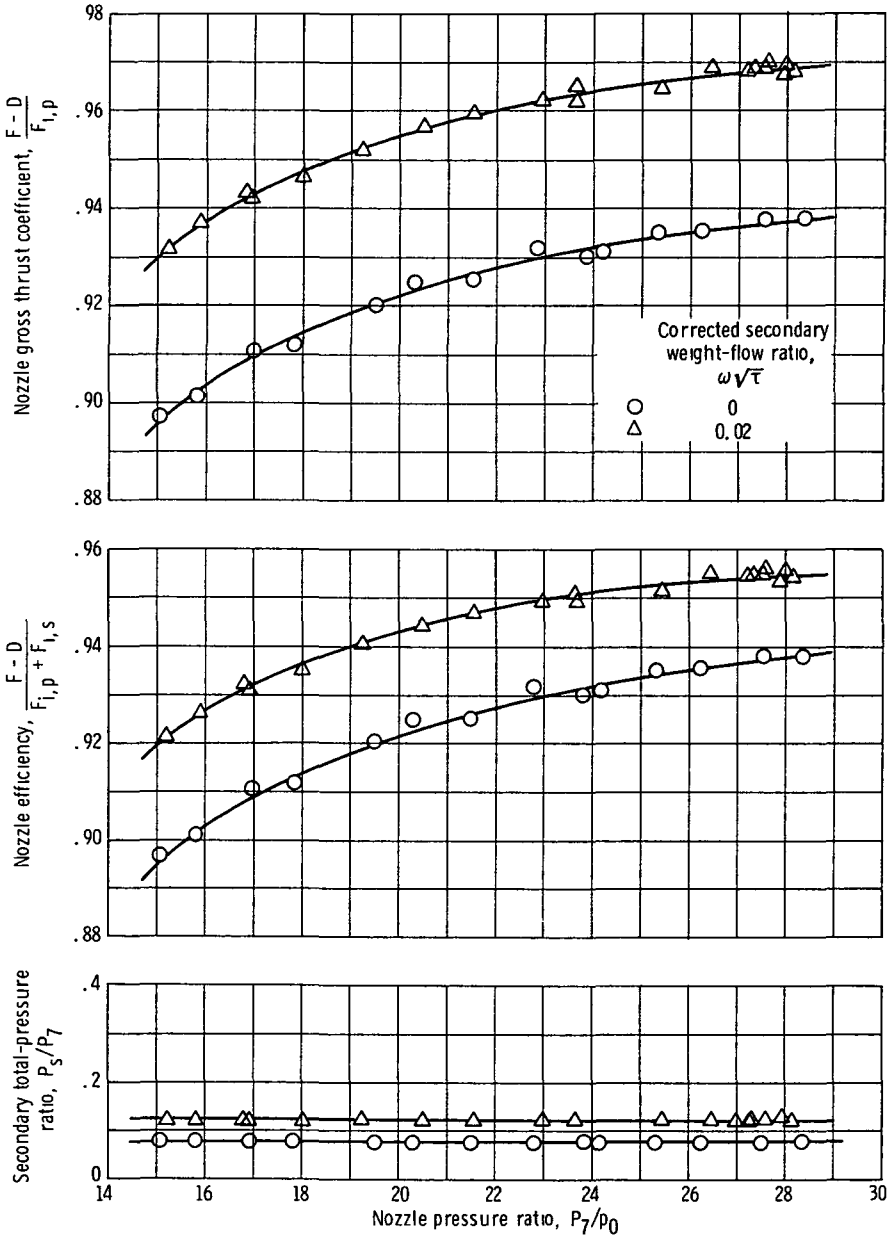

(c) 12-Spoke nozzle, shroud $x/d_{max} = 0.741$.

Figure 13. - Continued.

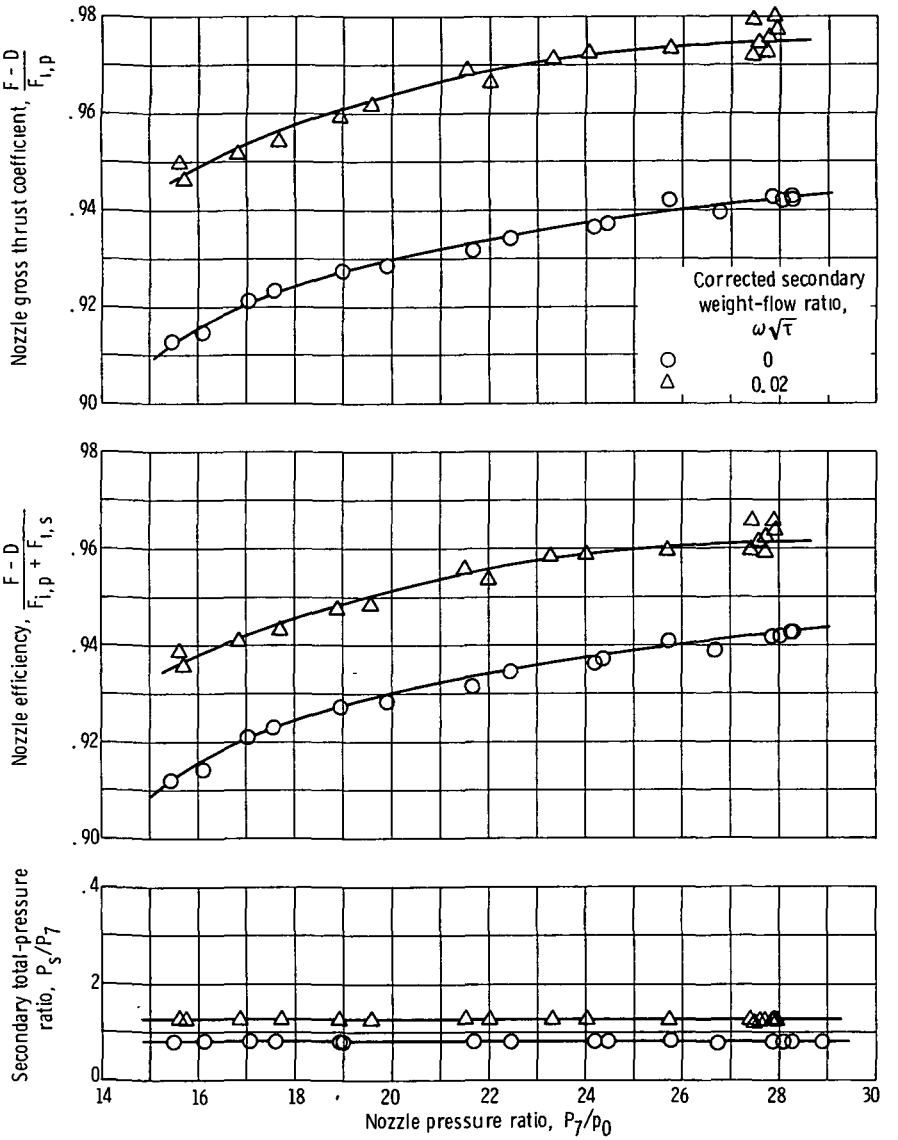

(d) 24-Spoke nozzle; shroud $x/d_{max} = 0.449$.

Figure 13. - Continued.

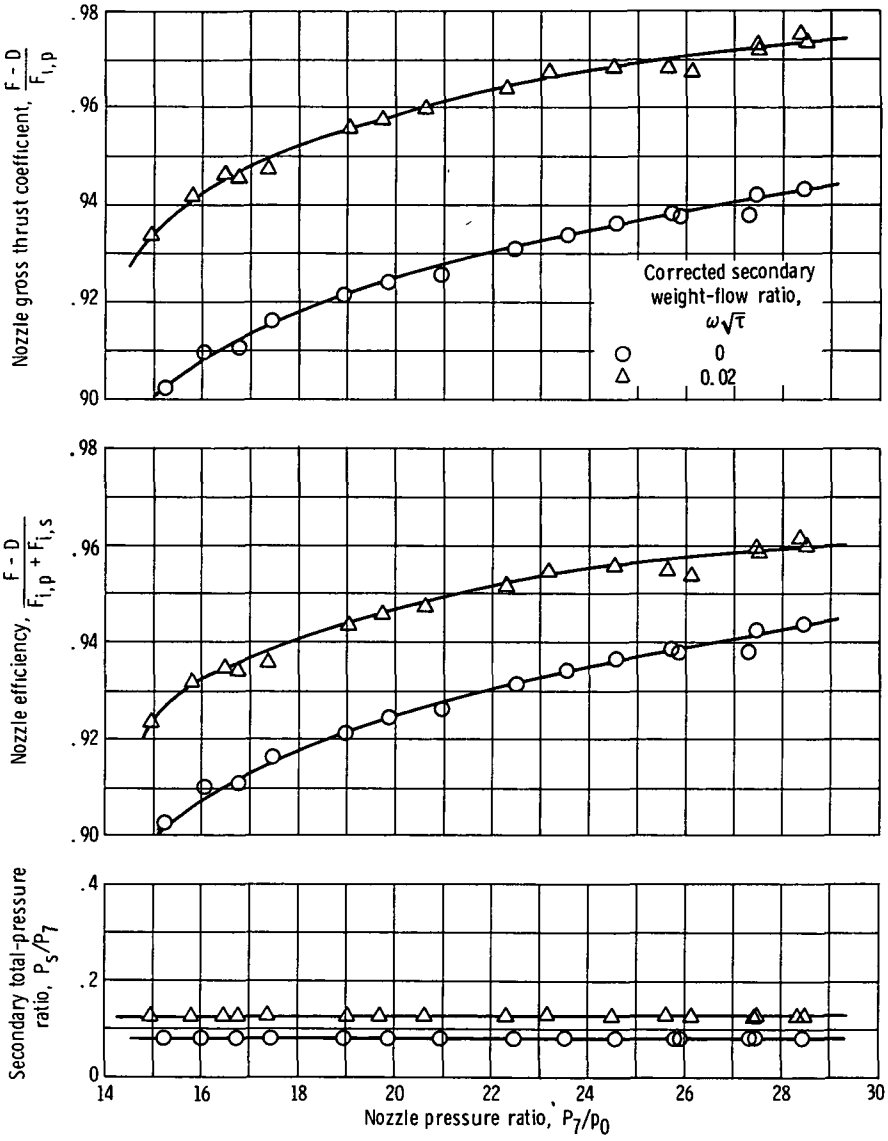

(e) 24-Spoke nozzle; shroud $x/d_{max} = 0.741$.

Figure 13. - Concluded.

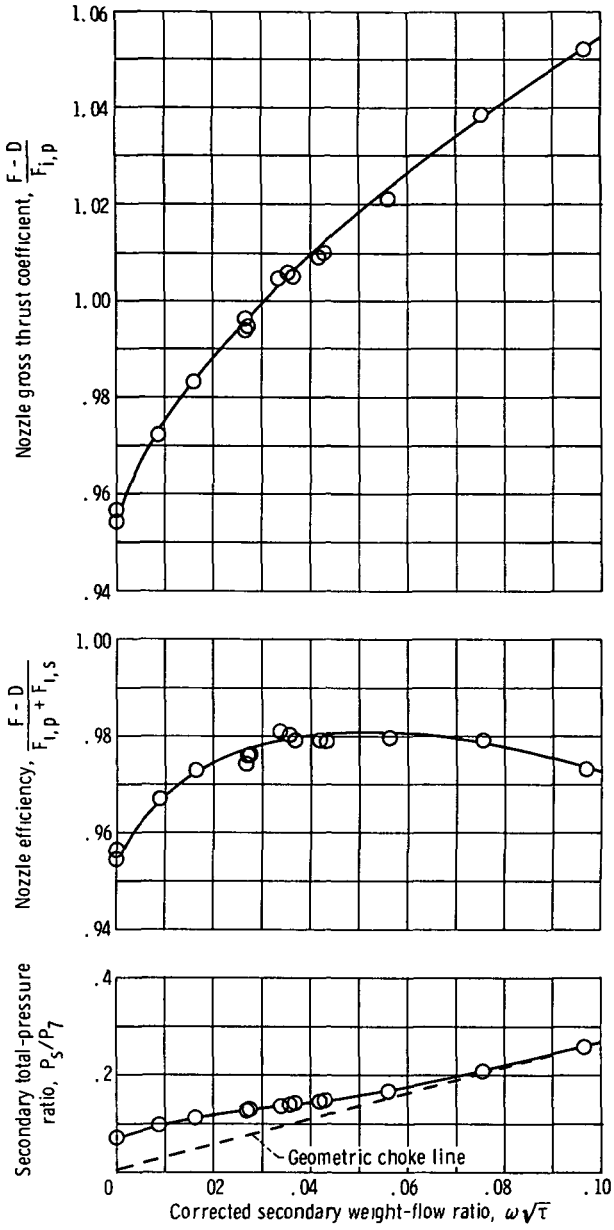

(a) Reference nozzle; shroud $x/d_{max} = 0.674$.

Figure 14. - Nozzle performance and pumping characteristics as functions of corrected secondary weight-flow ratio for supersonic-cruise configurations. Nozzle pressure ratio, 27.5.

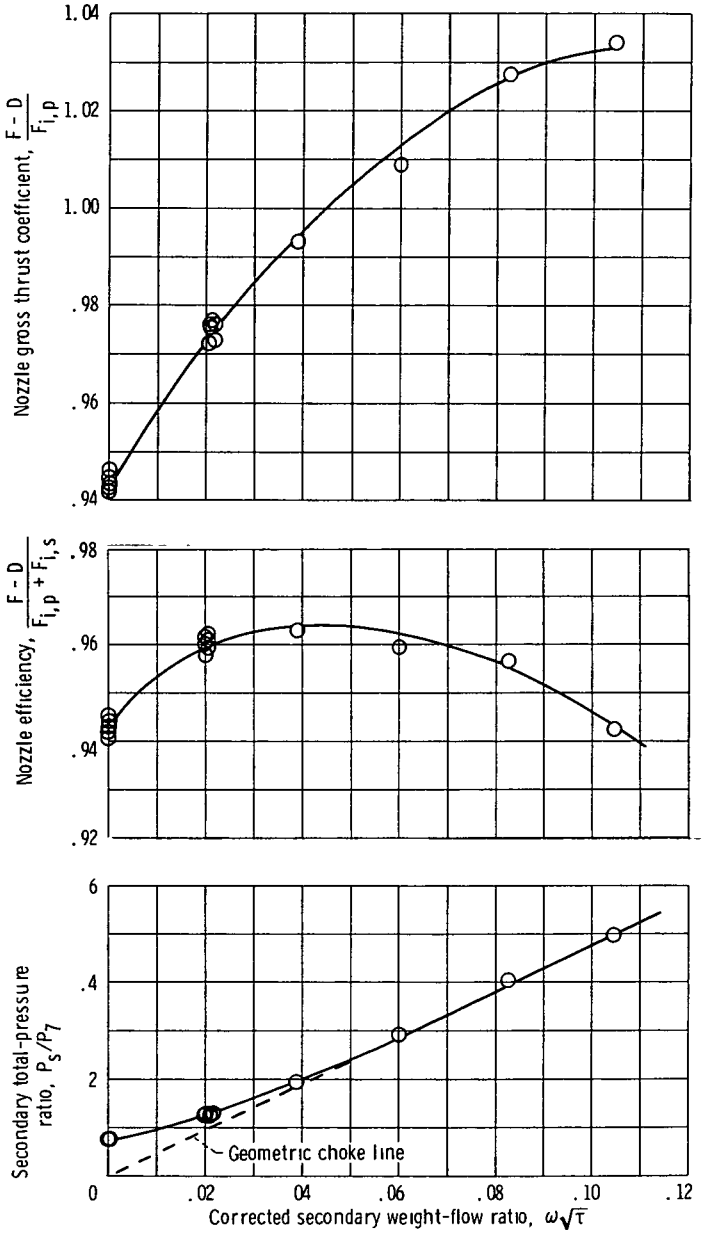

(b) 12-Spoke nozzle; shroud $x/d_{max} = 0.449$.

Figure 14. - Continued.

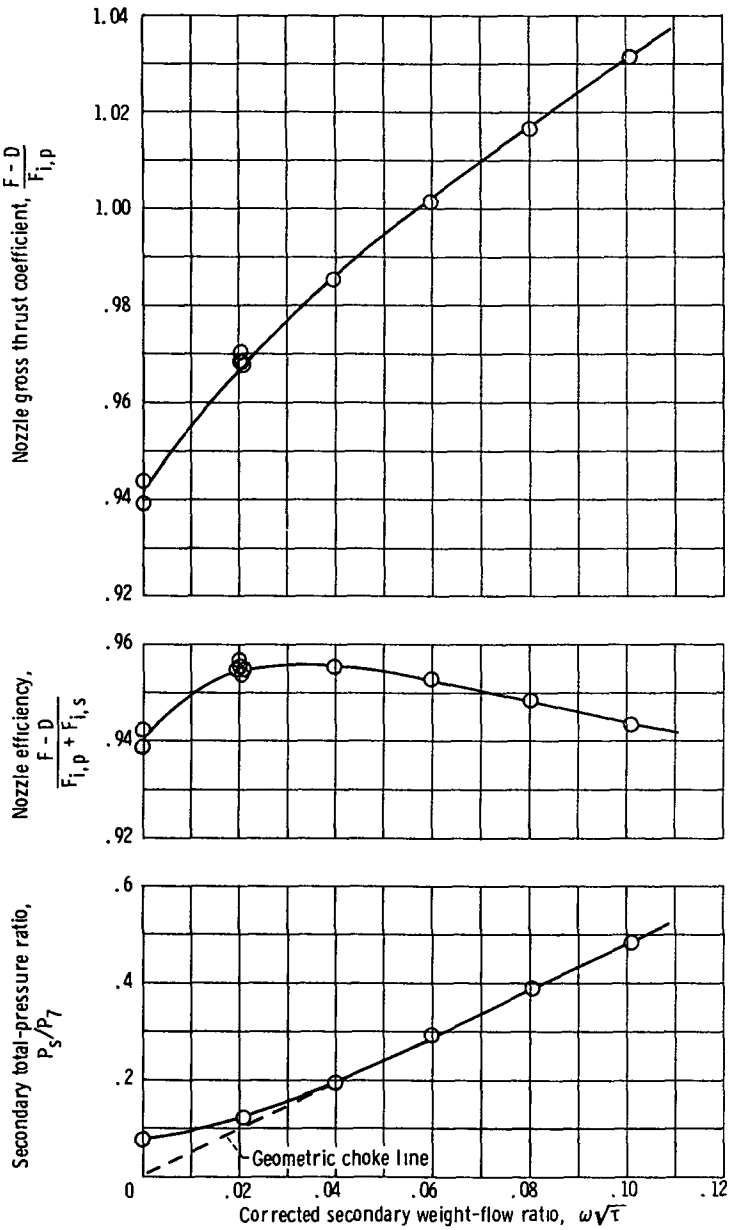

(c) 12-Spoke nozzle; shroud $x/d_{max} = 0.741$.

Figure 14. - Continued.

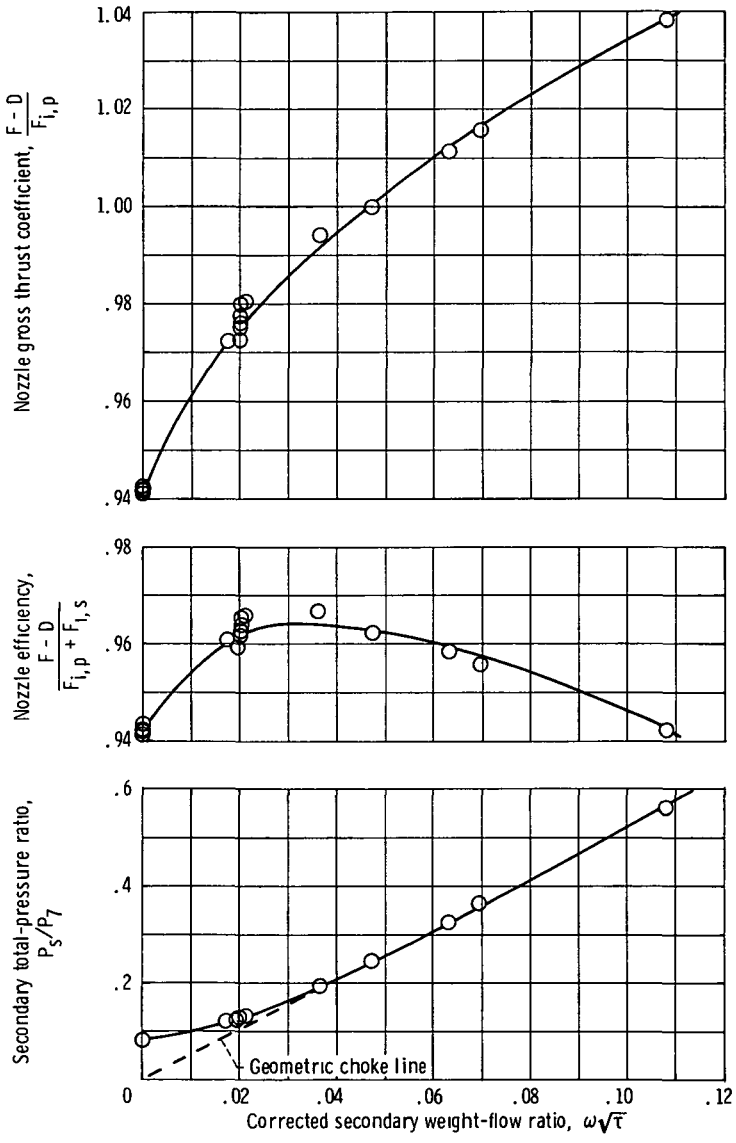

(d) 24-Spoke nozzle, shroud $x/d_{max} = 0.449$.

Figure 14. - Continued.

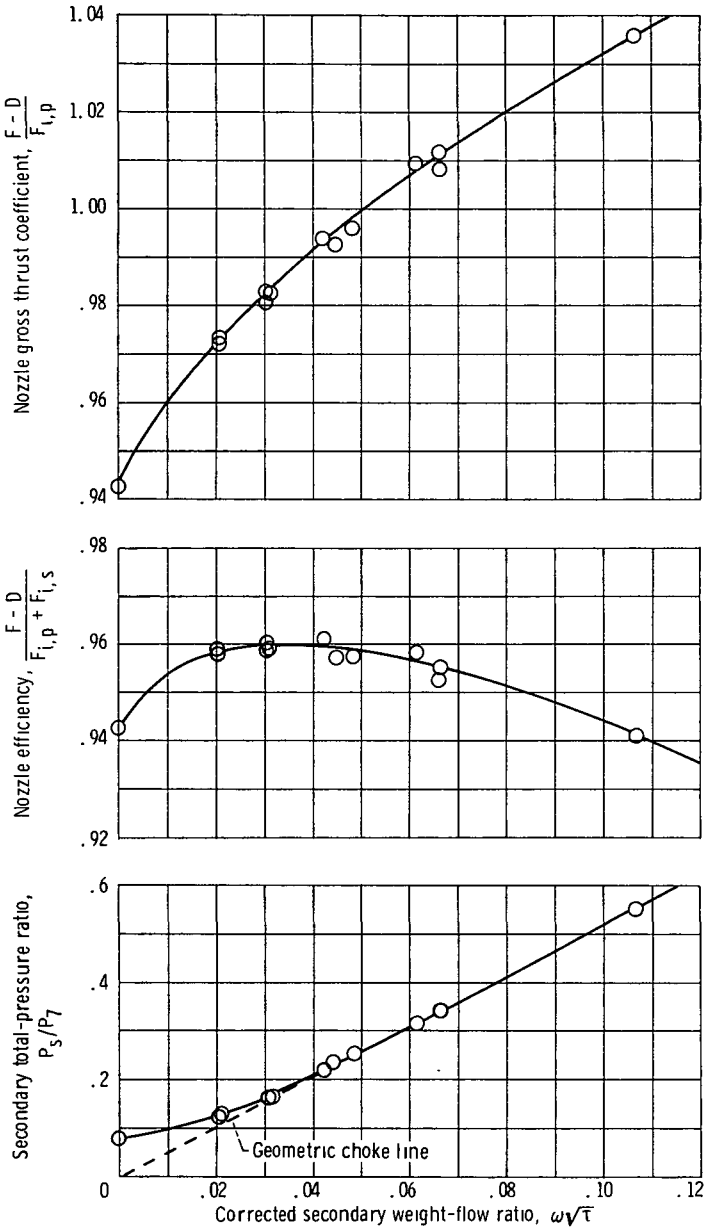

(e) 24-Spoke nozzle, shroud $x/d_{max} = 0.741$.

Figure 14 - Concluded.

NATIONAL AERONAUTICS AND SPACE ADMISTRATION
WASHINGTON, D.C. 20546

OFFICIAL BUSINESS
PENALTY FOR PRIVATE USE $300

FIRST CLASS MAIL

POSTAGE AND FEES PAID
NATIONAL AERONAUTICS AND
SPACE ADMINISTRATION

U.S.MAIL

NASA 451

POSTMASTER: If Undeliverable (Section 158 Postal Manual) Do Not Return

"The aeronautical and space activities of the United States shall be conducted so as to contribute . . . to the expansion of human knowledge of phenomena in the atmosphere and space. The Administration shall provide for the widest practicable and appropriate dissemination of information concerning its activities and the results thereof."

— NATIONAL AERONAUTICS AND SPACE ACT OF 1958

NASA SCIENTIFIC AND TECHNICAL PUBLICATIONS

TECHNICAL REPORTS: Scientific and technical information considered important, complete, and a lasting contribution to existing knowledge.

TECHNICAL NOTES: Information less broad in scope but nevertheless of importance as a contribution to existing knowledge.

TECHNICAL MEMORANDUMS: Information receiving limited distribution because of preliminary data, security classification, or other reasons.

CONTRACTOR REPORTS: Scientific and technical information generated under a NASA contract or grant and considered an important contribution to existing knowledge.

TECHNICAL TRANSLATIONS: Information published in a foreign language considered to merit NASA distribution in English.

SPECIAL PUBLICATIONS: Information derived from or of value to NASA activities. Publications include conference proceedings, monographs, data compilations, handbooks, sourcebooks, and special bibliographies.

TECHNOLOGY UTILIZATION PUBLICATIONS: Information on technology used by NASA that may be of particular interest in commercial and other non-aerospace applications. Publications include Tech Briefs, Technology Utilization Reports and Technology Surveys.

Details on the availability of these publications may be obtained from:

SCIENTIFIC AND TECHNICAL INFORMATION OFFICE

NATIONAL AERONAUTICS AND SPACE ADMINISTRATION

Washington, D.C. 20546